Universiteit
Leiden
The Netherlands

PI3K signaling and adherens junctions in invasive lobular breast cancer

Klarenbeek, S.

Citation

Klarenbeek, S. (2021, April 15). *PI3K signaling and adherens junctions in invasive lobular breast cancer*. Retrieved from https://hdl.handle.net/1887/3154437

Version:	Publisher's Version
License:	Licence agreement concerning inclusion of doctoral thesis in the Institutional Repository of the University of Leiden
Downloaded from:	https://hdl.handle.net/1887/3154437

Note: To cite this publication please use the final published version (if applicable).

Cover Page

Universiteit Leiden

The handle http://hdl.handle.net/1887/3154437 holds various files of this Leiden University dissertation.

Author: Klarenbeek, S.
Title: PI3K signaling and adherens junctions in invasive lobular breast cancer
Issue date: 2021-04-15

Loss of p120-catenin induces metastatic progression of breast cancer by inducing anoikis resistance and augmenting growth factor receptor signaling

Ron C.J. Schackmann[1,2,#], Sjoerd Klarenbeek[4,#], Eva J. Vlug[1], Suzan Stelloo[1], Miranda van Amersfoort[1], Milou Tenhagen[1], Tanya M. Braumuller[4], Jeroen F. Vermeulen[1], Petra van der Groep[1,3], Ton Peeters[1], Elsken van der Wall[3], Paul J. van Diest[1], Jos Jonkers[4] and Patrick W.B. Derksen[1,2]

[#] contributed equally

[1] Department of Pathology, University Medical Center Utrecht, Utrecht

[2] Cancer Center, University Medical Center Utrecht, Utrecht

[3] Division of Internal Medicine, University Medical Center Utrecht, Utrecht

[4] Division of Molecular Pathology and Cancer Systems Biology Center, The Netherlands Cancer Institute, Amsterdam, the Netherlands

Cancer Research 73, 4937-4949 (2013)

ABSTRACT

Metastatic breast cancer remains the chief cause of cancer-related death among women in the Western world. Although loss of cell–cell adhesion is key to breast cancer progression, little is known about the underlying mechanisms that drive tumor invasion and metastasis. Here, we show that somatic loss of p120-catenin (p120) in a conditional mouse model of noninvasive mammary carcinoma results in formation of stromal-dense tumors that resemble human metaplastic breast cancer and metastasize to lungs and lymph nodes. Loss of p120 in anchorage-dependent breast cancer cell lines strongly promoted anoikis resistance through hypersensitization of growth factor receptor (GFR) signaling. Interestingly, p120 deletion also induced secretion of inflammatory cytokines, a feature that likely underlies the formation of the prometastatic microenvironment in p120-negative mammary carcinomas. Our results establish a preclinical platform to develop tailored intervention regimens that target GFR signals to treat p120-negative metastatic breast cancers.

INTRODUCTION

Adherens junctions are required to maintain epithelial tissue integrity. They are established by homotypic interactions between E-cadherin (*CDH1*) molecules, which in turn control binding of cytosolic catenins that provide linkage to and regulation of the microtubule and actin cytoskeleton (1). Loss or temporal downregulation of E-cadherin is strongly linked to tumor development and progression of several cancer types (2). In breast cancer, timing of adherens junction inactivation has considerable impact on tumor etiology and cellular biochemistry. Although mutational inactivation of E-cadherin is an initiating and causal event in the development of invasive lobular carcinoma (ILC; refs. 3–5), late epigenetic silencing may underlie the progression of invasive ductal carcinoma (IDC; ref. 6) in a process called epithelial-to-mesenchymal transition (EMT; ref. 7). In conjunction with this is the finding that while translocation of p120-catenin (p120; *CTNND1*) upon E-cadherin inactivation controls Rock-dependent metastasis of ILC, IDC cells do not show dependency on this pathway (8, 9). Thus, p120 may play context-dependent roles in the development and progression of breast cancer.

Under physiologic conditions, p120 binds to the intracellular juxtamembrane domain of E-cadherin (10). Here, p120 controls E-cadherin stability and turnover in a process mediated by Hakai (*CBLL1*), (11), presenilin-1 (*PSEN1*; ref. 12), and/or Numb (*NUMB*; ref. 13). Others and we have shown that genetic ablation of E-cadherin or p120 in mouse mammary epithelial cells results in the induction of apoptosis, indicating that inactivation of adherens junction function is not tolerated in the mammary gland (4, 14, 15). In contrast, genetic inactivation in other organ systems does not induce cell death, but instead induces impaired tissue homeostasis and hyperplasia (16–19). Also, p120 inactivation in mice seems to result in inflammation, which may be caused by a loss of barrier function and the production of inflammatory chemoattractants (17, 18, 20). Interestingly, recent data showed that p120 can function as a *bona fide* tumor suppressor in the upper gastrointestinal tract. Here, somatic p120 inactivation induced the development of squamous cell carcinoma, which was accompanied by autocrine production of monocyte/macrophage attractants, thus promoting a proinvasive tumor microenvironment (21).

Several studies have indicated that p120 may be lost or inactivated in approximately 10% of IDC breast cancers cases. Loss was defined as absence of expression in more than 10% of the tumor cells, and correlated to absence of progesterone receptor (PGR) expression and poor prognosis (22–24). Here, we have analyzed p120 expression in a comprehensive set of human invasive breast cancer samples and

studied the consequences of inactivation of p120 in mammary tumor development and progression in the context of p53 (*Trp53*) loss using conditional mouse models. Mammary-specific p120 loss in mice resulted in a switch from noninvasive to metastatic mammary carcinoma that phenotypically resembled human metaplastic breast cancer. Furthermore, inactivation of p120 resulted in anoikis resistance, which was exacerbated by a sensitization to growth factor receptor (GFR) signaling due to inactivation of the adherens junction. Finally, we show that loss of p120 results in secretion of inflammatory cytokines, which may promote formation of a prometastatic tumor microenvironment.

MATERIALS AND METHODS

Additional experimental procedures are described in detail in the Supplementary Experimental Procedures.

Patient material

Of note, 298 cases of IDC were collected and histologically examined as described in the Supplementary Experimental Procedures.

Antibodies and cytokine array

The following antibodies were used: mouse anti-p120 [Western blot (WB), 1:2,000; immunofluorescence (IF), 1:500; IHC, 1:500; clone 98/pp120; BD Biosciences], tetramethyl-rhodamin-conjugated p120 (immunofluorescence, 1:150; BD Biosciences) mouse anti-E-cadherin (WB, 1:2,000; clone 36/E-cadherin; BD Biosciences), fluorescein isothiocyanate (FITC)-conjugated E-cadherin (IF, 1:150; BD Biosciences), mouse anti-E-cadherin (IHC, 1:200; clone 4A2C7; Zymed, Invitrogen), rat anti-CK 8 (Troma-1; IHC, 1:125; Developmental Studies Hybridoma Bank products), rabbit anti-CK14 (IHC, 1:10,000; BabCo), guinea pig anti-vimentin (IHC, 1:400; RDI), rabbit anti-SMA (IHC, 1:350; Lab Vision), rat anti-mouse F4/80 (IHC, 1:300; Serotec), mouse anti-β-catenin (WB, 1:2,000; BD Biosciences), rabbit anti-αE-catenin (WB, 1:2,000; Sigma) goat anti-AKT1 (C-20; WB, 1:1,000; Santa Cruz Biotechnology), rabbit anti-p-AKT1^{s473} (WB, 1:1,000; Cell Signaling Technology), rabbit anti-ERK2 (C-14; Santa Cruz Biotechnology), rabbit anti-p-MAPK (p44/42; WB, 1:2,000; Cell Signaling Technology), mouse anti-RhoA (WB, 1:250; Santa Cruz Biotechnology), mouse anti-Rac1 (WB, 1:1,000; Upstate), rabbit anti-Cdc42 (WB, 1:250; Santa Cruz Biotechnology), rabbit anti-EGFR (WB, 1:500; Cell Signaling Technology), rabbit anti-p-EGFR^{T1068} (WB, 1:1,000; Cell Signaling Technology), and sheep anti-digoxigenin (Roche). Secondary antibodies: horseradish peroxidase

(HRP)–conjugated rabbit anti-goat, goat anti-mouse, (1:2,000; Dako), HRP-conjugated goat anti-rabbit (1:2,000; Cell Signaling Technology), rabbit anti-sheep antibodies (Dako), Alexa Fluor 561–conjugated anti-mouse antibodies (Molecular Probes), goat anti-rat Alexa Fluor 488 (Invitrogen), goat anti-rabbit Alexa Fluor 555 (Invitrogen), biotin-conjugated anti-guinea pig (Jackson ImmunoResearch). Biotin label-based mouse antibody array was used according to the manufacturer's recommendations (RayBiotech AAM-BLM-1-4).

Mouse crossings genotyping and generation of cell lines

p120 conditional mice containing *loxP* sites in intron 2 and 8 of *Ctnnd1*, (Black-swiss;129SvEvTac; ref. 17) were a kind gift from Al Reynolds (Vanderbilt University Medical Center, Nashville, TN) and crossed onto the *Wcre;Trp53*$^{F/F}$ mouse model (FVB/N;Ola129/sv; refs. 4, 5). Cohorts of *Wcre;Ctnnd1*$^{F/+}$*;Trp53*$^{F/F}$ and *Wcre;Ctnnd1*$^{F/F}$*;Trp53*$^{F/F}$ mice were bred from the resulting offspring. *Wcre;Ctnnd1*$^{F/+}$*;Trp53*$^{F/F}$ mice were subsequently used to generate *Wcre;Trp53*$^{F/F}$ mice to control for the introduction of Black-swiss;129SvEvTac genetic material. Mice were bred and maintained on a mixed background of (FVB/N;Ola129/sv). Genotyping was done by PCR as described previously (4, 17). Mice were monitored for the development of mammary tumors by palpation and euthanized by CO_2 inhalation when mammary tumor size reached a diameter of 10 mm. Full autopsies were conducted for the analysis of tumor histology and the detection of metastases. Age at the time of euthanasia was used to generate the tumor-free survival curves. For the generation of tumor cell lines, tumors from *Wcre;Ctnnd1*$^{F/F}$*;Trp53*$^{F/F}$ animals were extracted, minced by hand using scalpel blades, and plated onto regular culture dishes in Dulbecco's Modified Eagle Medium (DMEM)-F12 medium as described previously (5).

Plasmids

For stable knockdown of p120, previously described sequences were cloned into a doxycycline-inducible lentiviral expression system (8). For p120 reconstitution experiments, a lentiviral p120-1A cDNA expression construct was generated as described in the Supplementary Experimental Procedures.

Virus production and Rho GTP pulldown

Lentivirus production and transductions were done as described previously (5). In short, 10^6 Cos-7 cells were seeded onto 10-cm Petri dishes and transiently transfected after 24 hours with third-generation packaging constructs (25) and the indicated viral construct

using X-tremeGENE 9 reagent (Roche). Pull-down assays for GTP-loaded RhoGTP family members were conducted as described previously (8, 26).

Cell culture

Mouse Trp53$^{\Delta/\Delta}$-7 (WP6) and Trp53$^{\Delta/\Delta}$-3 (KP6) cell lines were generated from primary tumors that developed in *Wcre;Trp53$^{F/F}$* and *K14cre;Trp53$^{F/F}$* female mice, respectively. Cells were cultured as described previously (5). Human breast cancer cell lines T47D and MCF7 were cultured in DMEM-F12 (Invitrogen) containing 6% fetal calf serum, 100 IU/mL penicillin, and 100 µg/mL streptomycin. T47D and MCF7 cell lines were obtained from American Type Culture Collection. Authenticity was tested on May 16, 2012 by means of short-tandem repeat (STR) profiling (LGC Standards), after which large quantities of cells were frozen separately.

Western blot analysis, immunohistochemistry, and fluorescence

Western blotting was conducted as described previously (27). For immunohistochemistry and fluorescence, tissues and cells were isolated, fixed, and stained as described in the Supplementary Experimental Procedures. *In situ* hybridization–IHC double staining experiments were carried out using labeled PCR products to identify EGF mRNA as described in the Supplementary Experimental Procedures. Samples were analyzed using a DeltaVision RT system (Applied Precision), equipped with a CoolSnap HQ camera and SoftWorx software. Maximum projections were taken from a stack of deconvolved images.

Anoikis resistance and FACS analysis

Anoikis resistance was analyzed by seeding cells at a density of 20,000 cells per well (in 500 µL) in a 24-well ultra-low cluster polystyrene culture dish (Corning). After 4 days, cells were harvested and resuspended in 75 µL of Annexin V buffer supplemented with Annexin V (IQ Products) and propidium iodide (Sigma-Aldrich). The percentage of anoikis-resistant cells was defined as the Annexin V and propidium iodide–negative population analyzed on a BD FACSCalibur. To determine cellular EGF-binding ability, 400 ng of Alexa Fluor 647–conjugated EGF (Invitrogen) was incubated with 1×10^5 trypsinized ice-cold cells in 100 µL PBS. Cells were washed with PBS to remove unbound EGF-647 and subjected to fluorescence-activated cell sorting (FACS) analysis.

Growth factor stimulation assays

Cells were seeded at 400,000 cells per 6-well in growth factor–free medium for 4 hours, subsequently washed and serum-starved overnight. Next, cells were stimulated with

EGF (5 ng/mL; Sigma) or HGF (25 ng/mL; R&D Systems) for 10 minutes. Cells were placed on ice and washed twice with ice-cold PBS containing Ca^{2+} and Mg^{2+}, and directly lysed in lysis buffer.

Statistical analyses

Statistical analyses were conducted using GraphPad Prism 5 (GraphPad Software). Analyses on human samples were conducted as described previously (28). For analysis of growth pattern and metastasis formation, Fisher exact test was used. For metastasis-free survival analysis, the log-rank test was used. For anoikis assays, statistical significance was calculated using the Student *t* test (two-tailed), showing measurements of at least three independent experiments. Error bars in all experiments represent SD or SEM as indicated, of at least triplicate measurements. We considered *P* values less than 0.05 as statistically significant.

Ethics statement

All animal experiments were approved by the University Animal Experimental Committee, University Medical Center Utrecht (Utrecht, the Netherlands). Use of anonymous or coded leftover material for scientific purposes is part of the standard treatment contract with patients in our hospitals.

RESULTS

Loss of p120 expression in invasive breast cancer

To extend previous findings on loss of p120 expression in breast cancer, we conducted immunohistochemistry (IHC) on a panel of 298 invasive ductal breast cancers and determined their clinicopathologic variables (Supplementary Table S1). Membranous p120 was scored (absent/low vs. medium/high) in three independent tissue cores per tumor. Because we hypothesized that loss of p120 may be linked to increased tumor progression, we defined expression as absent/low if more than 10% of the tumor cells were negative for p120 (Supplementary Fig. S1A), as has been used for E-cadherin (29). Using these parameters, we observed that 34% of the IDC samples showed absent/low p120 staining. Upon correlation of p120 expression levels to clinicopathologic variables, a significant association was obtained between p120 loss, high tumor grade ($P = 0.007$), mitotic index (MAI; $P = 0.002$), and overall absence of hormone receptor expression ($P = 0.039$; Supplementary Table S2). Although p120 expression levels did not associate with tumor size, lymph node status, or the other clinicopathologic variables tested

(Supplementary Table S2), these data suggest that loss of p120 expression coincides with breast cancer aggressiveness.

Somatic inactivation of p120 results in the formation of metastatic mammary carcinoma

Functional inactivation of the adherens junction through somatic inactivation of E-cadherin is a causal event in the development of ILC (5). In E-cadherin–mutant breast cancer, p120 translocates to the cytosol where it exerts a key oncogenic role by regulating anchorage-independent tumor growth and metastasis (8). To study the effect of p120 loss on tumor development and progression of breast cancer, we introduced a conditional p120 allele (*Ctnnd1*^{F}; ref. 17) onto the *Wcre;Trp53*$^{F/F}$ (4) noninvasive mammary carcinoma model to produce *Wcre;Ctnnd1*$^{F/+}$*;Trp53*$^{F/F}$ and *Wcre;Ctnnd1*$^{F/F}$*;Trp53*$^{F/F}$ mice. To correct for the differences in genetic background between the *Ctnnd1*^{F} (17) and the *Wcre;Trp53*$^{F/F}$ (FVB/N; 129P2/OlaHsd) mice, a control cohort was bred using *Wcre;Ctnnd1*$^{F/+}$*;Trp53*$^{F/F}$ litter mates to produce *Wcre;Trp53*$^{F/F}$. Next, females were monitored for spontaneous tumor development. In contrast to conditional inactivation of E-cadherin (4, 5), we observed that the median tumor-free latency (T_{50}) did not significantly change in either *Wcre;Ctnnd1*$^{F/+}$*;Trp53*$^{F/F}$ (T_{50} = 223 days) or *Wcre;Ctnnd1*$^{F/F}$*;Trp53*$^{F/F}$ female mice (T_{50} = 214 days) when compared with *Wcre;Trp53*$^{F/F}$ females (T_{50} = 213 days; P = 0.5006 and 0.5859, respectively; Fig. 1A; Table 1). Mammary tumors from *Wcre;Trp53*$^{F/F}$ females were morphologically typed as adenocarcinomas and carcinosarcomas, with expansive growth patterns, dense cellular sheets, and irregular bundles of polygonal to plump spindle-shaped cells (Table 1). Tumors that developed in *Wcre;Ctnnd1*$^{F/+}$*;Trp53*$^{F/F}$ and *Wcre;Ctnnd1*$^{F/F}$*;Trp53*$^{F/F}$ females showed a shift from expansive to invasive growth as compared with *Wcre;Trp53*$^{F/F}$ animals (P = 0.026 and 0.006, respectively; Table 1). In contrast to somatic E-cadherin inactivation and the development of ILC, both heterozygous and homozygous loss of p120 resulted in metaplastic tumor cells displaying a spindle cell morphology, often expressing vimentin with focal expression of cytokeratin (CK)8 or CK14, reminiscent of an EMT (Fig. 1B, top; Supplementary Table S3; Supplementary Fig. S1B). Tumors developed with high incidence multifocally in different mammary glands and were characterized by a more abundant and dense stromal microenvironment. Mammary tumors from *Wcre;Ctnnd1*$^{F/+}$*;Trp53*$^{F/F}$ females did not show LOH of the *Ctnnd1* locus, as tumors expressed membrane-localized p120 and E-cadherin (Fig. 1B, middle and Supplementary Table S3). Mammary tumors from *Wcre;Ctnnd1*$^{F/F}$*;Trp53*$^{F/F}$ females showed large cells with pleomorphic nuclei, coarsely clumped chromatin, and sparse cytoplasm. As expected, all tumors from *Wcre;Ctnnd1*$^{F/F}$*;Trp53*$^{F/F}$ female mice lacked expression of membranous p120 and E-cadherin (Fig. 1B, right and Supplementary Table S3).

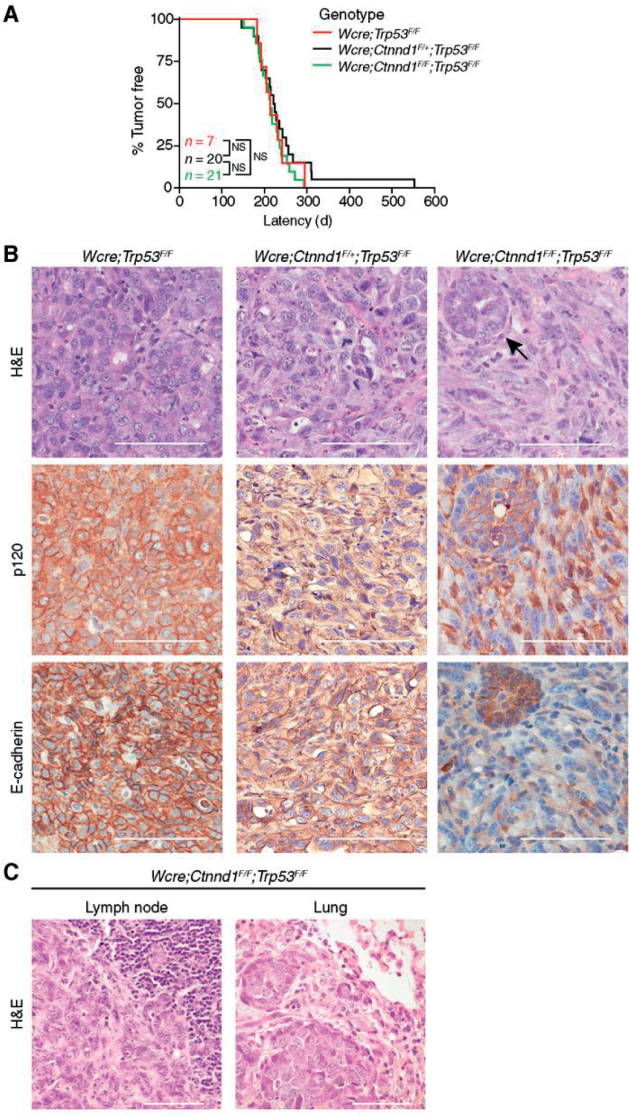

Figure 1. p120 is a metastasis suppressor in mammary carcinoma. A, conditional mammary-specific inactivation of p120 does not influence tumor-free latency. Kaplan–Meier tumor-free survival curves for *Wcre;Trp53*$^{F/F}$ (red line) versus *Wcre;Ctnnd1*$^{F/+}$*;Trp53*$^{F/F}$ (black line) versus *Wcre;Ctnnd1*$^{F/F}$*;Trp53*$^{F/F}$ (green line). Mice were sacrificed when tumors reached an average diameter of 10 mm. NS, not significant. B and C, loss of p120 induces a switch from nonmetastatic to metastatic mammary carcinoma. B, histopathology of consecutive sections from mammary tumors derived from *Wcre;Trp53*$^{F/F}$ (left), *Wcre;Ctnnd1*$^{F/+}$*;Trp53*$^{F/F}$ (middle), and *Wcre;Ctnnd1*$^{F/F}$*;Trp53*$^{F/F}$ (right). Shown are hematoxylin and eosin (H&E) staining and IHC for p120 and E-cadherin. Arrow in right panel points to a preexistent hyperplastic mammary duct. C, homozygous loss of p120 leads to metastasis. Examples of distant metastases from *Wcre;Ctnnd1*$^{F/F}$*;Trp53*$^{F/F}$ female animals showing disseminated tumor cells in a lymph node (left) and lungs (right). Bars, 100 µm.

Table 1. Mammary tumor spectrum of *Wcre;Trp53F/F*, *Wcre;Ctnnd1F/+;Trp53F/F* and *Wcre;Ctnnd1F/F;Trp53F/F* female mice

Genotype	Number of mice	Median latency, d	Metastasis	Local invasion	AC	SC/CS	mILC
Wcre;Trp53$^{F/F}$	7	213	0 (0%)	0 (0%)	3 (43%)	7 (100%)	0 (0%)
Wcre;Ctnnd1$^{F/+}$;Trp53$^{F/F}$	20	223	1 (5%)	10 (50%)	1 (5%)	19 (95%)	1 (5%)
Wcre;Ctnnd1$^{F/F}$;Trp53$^{F/F}$	21	214	9 (43%)	14 (67%)	3 (14%)	18 (86%)	1 (5%)

NOTE: If tumors were composed of two separate histologic types, both were counted separately.
Abbreviations: AC, adenocarcinoma, glandular-type mammary carcinoma; SC/CS, solid carcinoma/carcinosarcoma, tumor consisting of epithelial and mesenchymal cell types.

When compared with human breast cancer, tumors that developed in *Wcre;Trp53$^{F/F}$* mice corresponded to well-differentiated "luminal type" IDC, with low proliferation and expansive growth patterns. They predominantly express luminal CK8, showing little expression of basal CK14 (Supplementary Fig. S1B and Supplementary Table S3). Also, these tumors show a relatively good prognosis with infrequent formation of distant metastases. The highly infiltrative tumors arising in *Wcre;Ctnnd1$^{F/F}$;Trp53$^{F/F}$* females corresponded to poorly differentiated "basal type" tumors. As such, they presented phenotypic features resembling human metaplastic IDC that are characterized by a high proliferation rate, strong nuclear atypia, and expression of CK14 (*KRT14*) and vimentin (*VIM*). In contrast to ILC, mouse and human metaplastic tumors displayed decreased p120 levels and a punctate/mislocalized E-cadherin expression pattern (Supplementary Fig. S1C and Supplementary Table S3). Human metaplastic carcinoma corresponds with poor prognosis and rapid onset of distant metastases (30).

Interestingly, and in contrast to dual somatic inactivation of E-cadherin and p53 (4, 5), we observed abundant formation of precursor carcinoma *in situ* (CIS) lesions in *Wcre;Ctnnd1$^{F/F}$;Trp53$^{F/F}$* females (Fig. 2A). CIS lesions showed loss of p120, but occasionally retained low levels of E-cadherin expression (Fig. 2B and C), indicating that upon p120 inactivation residual E-cadherin remains expressed in a temporal manner, which may underlie the initial noninvasive nature of the CIS-type structures.

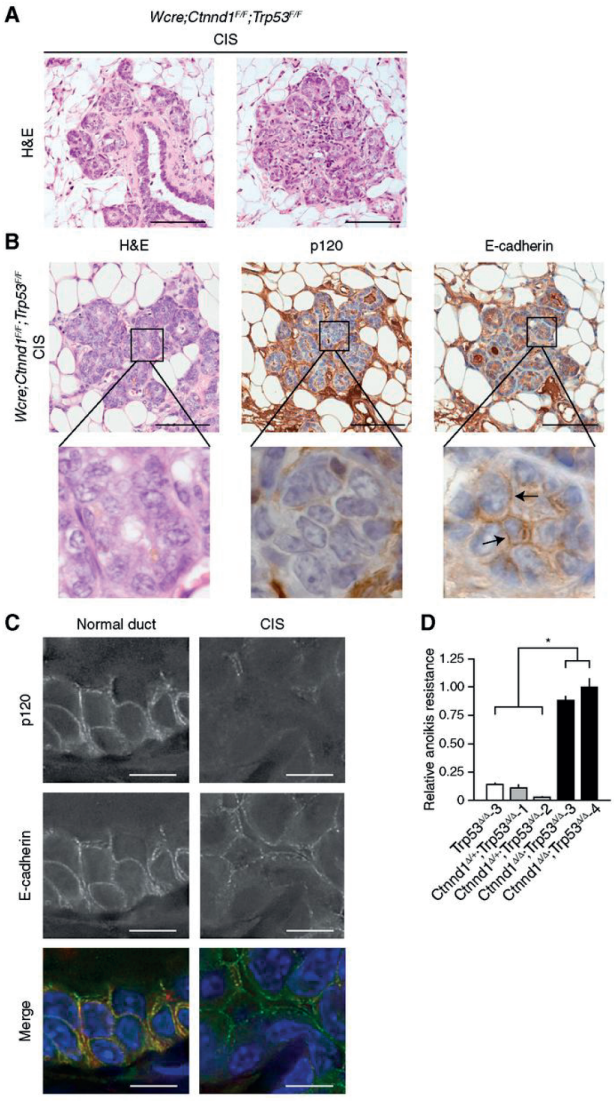

Figure 2. Somatic inactivation of p120 leads to development of CIS. A, CIS formation in premalignant *Wcre;Ctnnd1$^{F/F}$;Trp53$^{F/F}$* female mice. Shown are two separate hematoxylin and eosin (H&E) stainings. B and C, residual E-cadherin expression in CIS-type lesions in *Wcre;Ctnnd1$^{F/F}$;Trp53$^{F/F}$* female mice. B and C, H&E staining and IHC for p120 and E-cadherin on consecutive sections (B) and IF stainings for E-cadherin (green) and p120 (red) in a normal mammary duct (top) and a CIS-type mammary lesion (bottom) from a *Wcre;Ctnnd1$^{F/F}$;Trp53$^{F/F}$* female mouse (C). Note the presence of E-cadherin (arrows) in the absence of p120 expression. Bars, 10 μm. D, metastatic capacity correlates to anoikis resistance. Trp53$^{\Delta/\Delta}$ cell line (white bar) and primary cultures derived from tumors that developed in *Wcre;Ctnnd1$^{F/+}$;Trp53$^{F/F}$* (gray bars) and *Wcre;Ctnnd1$^{F/F}$;Trp53$^{F/F}$* (black bars) female mice were subjected to 4 days of anchorage independent culturing and subsequent anoikis resistance analysis using FACS. *, $P < 0.005$. Error bars represent SD of triplicate experiments.

Next, we examined whether the acquisition of invasive behavior upon p120 ablation resulted in an increased metastatic rate. We observed a significant increase in tumor cell dissemination in *Wcre;Ctnnd1$^{F/F}$;Trp53$^{F/F}$* versus *Wcre;Ctnnd1$^{F/+}$;Trp53$^{F/F}$* and *Wcre;Trp53$^{F/F}$* female mice (both $P < 0.05$; Table 1), a phenotype not observed in previously published models where inactivation was targeted to the gastrointestinal tract or skin (17, 18, 20, 21). Metastases phenotypically resembled the primary tumor and localized to regional or distant lymph nodes and lungs (Fig. 1C). Because tumor-free latency was identical in *Wcre;Ctnnd1$^{F/+}$;Trp53$^{F/F}$* versus *Wcre;Ctnnd1$^{F/F}$;Trp53$^{F/F}$* mice, but only *Wcre;Ctnnd1$^{F/F}$;Trp53$^{F/F}$* showed metastatic dissemination, we generated primary cultures from both tumor models and assayed anoikis resistance, a hallmark of metastatic cells (5, 31). In agreement with the *in vivo* metastatic behavior, we observed that tumor cells derived from *Wcre;Ctnnd1$^{F/F}$;Trp53$^{F/F}$* female mice (Ctnnd1$^{\Delta/\Delta}$;Trp53$^{\Delta/\Delta}$) were anoikis resistant, whereas neither cells derived from *Wcre;Ctnnd1$^{F/+}$;Trp53$^{F/F}$* nor *Wcre;Trp53$^{F/F}$* mammary tumors (Ctnnd1$^{\Delta/+}$;Trp53$^{\Delta/\Delta}$ and Trp53$^{\Delta/\Delta}$, respectively) survived under these conditions (Fig. 2D). These results suggested that homozygous inactivation of p120 is necessary for the acquisition of anchorage independence and subsequent dissemination of mammary tumor cells. In conclusion, we show that conditional loss of p120 induces a transition to highly invasive and metastatic mammary carcinoma.

Loss of p120 results in loss of the adherens junction, transition to a mesenchymal phenotype, and anoikis resistance

Because we observed anoikis resistance in primary tumor cells derived from *Wcre;Ctnnd1$^{F/F}$;Trp53$^{F/F}$* female mice (Fig. 2D), we examined if p120 inactivation was the causal event in this anchorage-independent survival phenotype. To this end, we made use of Trp53$^{\Delta/\Delta}$ tumor cell lines previously generated from adenocarcinomas that developed in either *K14Cre;Trp53$^{F/F}$* (32) or *Wcre;Trp53$^{F/F}$* female mice (4). Two independent Trp53$^{\Delta/\Delta}$ cell lines were transduced using a doxycycline-inducible lentiviral construct targeting p120 (p120-iKD). Doxycycline administration resulted in a strong reduction of p120 protein expression (Fig. 3A), which was accompanied by a decrease in both E-cadherin and β-catenin levels and a slight decrease in α-catenin protein expression (Supplementary Fig. S2A and S2B). Upon p120-iKD, cells lost their typical epithelial appearance and transitioned toward a mesenchymal and motile phenotype (Supplementary Fig. S2F). To confirm the specificity of the RNA interference (RNAi) sequence used, we reconstituted cells with a nontargetable p120 cDNA to near endogenous levels, which completely reverted the doxycycline-induced EMT phenotype (Fig. 3A and Supplementary Fig. S2E and S2F).

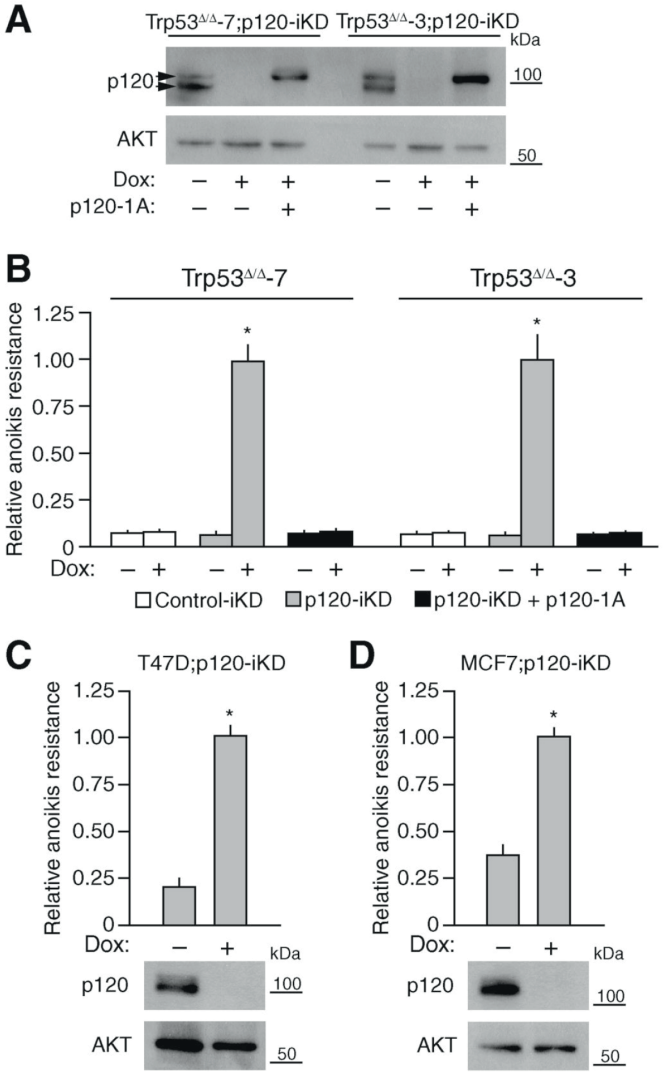

Figure 3. Loss of p120 results in anoikis resistance of E-cadherin–expressing breast cancer cells. A, two independent Trp53$^{\Delta/\Delta}$ cell lines were transduced with viruses carrying doxycycline (Dox)-inducible p120 short hairpin RNAs (shRNA; p120-iKD) and a nontargetable p120 isoform1A (p120-1A). Shown is the extent of p120 knockdown and p120-1A expression levels. Arrows indicate p120 isoforms. AKT was used as a loading control. B, Trp53$^{\Delta/\Delta}$;Control-iKD-, p120-iKD-, and p120-1A–expressing mammary carcinoma cells were cultured in the presence or absence of doxycycline for 4 days before subjecting cells to 4 days of anchorage-independent culturing and subsequent anoikis resistance analysis using FACS. C and D, T47D (C) and MCF7 (D) were transduced with viruses carrying p120-iKD constructs targeting human p120, treated with doxycycline for 4 days, and subjected to nonadherent culturing. Anoikis resistance was analyzed after 4 days. Bottom, the extent of p120 knockdown (top blot). AKT was used as loading control (bottom blot). *, $P < 0.005$. Error bars represent SD of triplicate experiments.

We next cultured two independent Trp53$^{\Delta/\Delta}$;p120-iKD cell lines in suspension and assayed anoikis resistance in the presence and absence of doxycycline. Although the majority of untreated Trp53$^{\Delta/\Delta}$;p120-iKD cells underwent anoikis, administration of doxycycline-induced anoikis resistance (Fig. 3B), which could be fully reverted upon expression of a nontargetable p120 construct (Fig. 3B). To substantiate these findings, we used two E-cadherin–expressing and anchorage-dependent human breast cancer cell lines (T47D and MCF7) in which we conducted knockdown of p120 and assayed anchorage independence. MCF7 was previously reported to acquire anchorage independence in soft agar upon constitutive p120 KD (9). Indeed, as for the mouse mammary carcinoma cells, p120-iKD induced downregulation of the adherens junction members and functionally induced anoikis resistance (Supplementary Fig. S2C and S2D and Fig. 3C and D). In conclusion, our data show that p120 knockdown results in loss of adherens junction function, and suggests that this underlies acquisition of anoikis resistance. Because these features are well-known hallmarks of malignancy (33), our findings suggest that loss of p120 may lead to metastasis through acquisition of anchorage independence.

Loss of p120 potentiates GFR signaling

Upon knockdown of p120 in MCF7, cells acquire Rac-dependent anchorage-independent survival, which is probably due to relieve of E-cadherin–mediated inhibition of Ras (*KRAS*; ref. 9). Although we could confirm that active Rac1 (*RAC1*) levels increased in MCF7 upon p120-iKD, we did not detect activation of Rac1 in either Trp53$^{\Delta/\Delta}$;p120-iKD cell lines or human T47D;p120-iKD cells after doxycycline administration (Supplementary Fig. S3). Also, no changes were observed in the levels or activity of the other Rho family members RhoA (*RHOA*) and Cdc42 (*CDC42*; Supplementary Fig. S3C), indicating that loss of p120 in these cell systems does not result in aberrant Rho GTPase activation.

Formation or functional disruption of adherens junctions can affect EGF receptor (EGFR) activity (34). Whether adherens junction disruption results in activation or inhibition of EGFR seems to be largely cell type–dependent (35, 36). Because p120 knockdown resulted in a loss of adherens junction formation through downregulation of E-cadherin, we wondered whether GFR signaling was affected. To this end, we stimulated doxycycline-treated Trp53$^{\Delta/\Delta}$;p120-iKD cells with EGF and assayed EGFR phosphorylation. Although EGF stimulation in control-iKD cells induced a modest EGFR tyrosine phosphorylation, knockdown of p120 resulted in a 1.5- to 2.0-fold increased phosphorylation (Fig. 4A, compare lanes 3 and 4; quantification of three independent experiments in Fig. 4B; nonstimulated in Supplementary Fig. S5A). In

line with these findings, we observed that the downstream PI3K/AKT and mitogen-activated protein kinases (MAPK) pathways displayed a 3- to 5-fold increased EGF-induced phosphorylation upon knockdown of p120 (Fig. 4A and B). To substantiate these findings, we made use of the Ctnnd1$^{\Delta/\Delta}$;Trp53$^{\Delta/\Delta}$ cell lines. Similarly to the GFR sensitization after inducible p120 knockdown, Ctnnd1$^{\Delta/\Delta}$;Trp53$^{\Delta/\Delta}$ cells showed a robust increase in EGF-induced phosphorylation of EGFR and MAPK and a modest induction of phosphorylated AKT as compared with Trp53$^{\Delta/\Delta}$ cells (Supplementary Fig. S6A). Furthermore, EGF stimulation of MCF7;p120-iKD cells also showed a sensitization of EGFR, AKT, and MAPK phosphorylation upon knockdown of p120 (Fig. 4C and D). The increased EGFR signaling following p120 knockdown was not due to increased EGFR levels or EGF binding at the plasma membrane (Fig. 4A and Supplementary Fig. S5C). However, we cannot exclude that p120 knockdown induced autocrine activation of GFR signaling in the presence of anchorage, as serum starvation resulted in low levels of activated EGFR, AKT, and MAPK signaling (Supplementary Fig. S5A and S5B). To determine whether the sensitized GFR signaling was EGFR-specific, we also stimulated the cells with hepatocyte growth factor (HGF) to activate the receptor tyrosine kinase MET. In line with the effects on EGF-dependent signaling, we observed a marked increase of AKT and MAPK phosphorylation upon p120 knockdown and subsequent HGF treatment of mouse and human cells (Supplementary Fig. S4A–S4C), indicating that p120-controlled GFR signaling is a general mechanism. To validate whether the increased GFR sensitivity also occurred *in vivo*, we investigated the expression of p-AKT and p-MAPK in tumors from *Wcre;Trp53$^{F/F}$;Ctnnd1$^{F/F}$* and *Wcre;Trp53$^{F/F}$* female mice. Indeed, loss of p120 induced activation of AKT, and to a lesser extent MAPK signals (Supplementary Fig. S6C). In conclusion, our data imply that loss of p120 leads to an increased sensitization of GFR signaling in breast cancer cells.

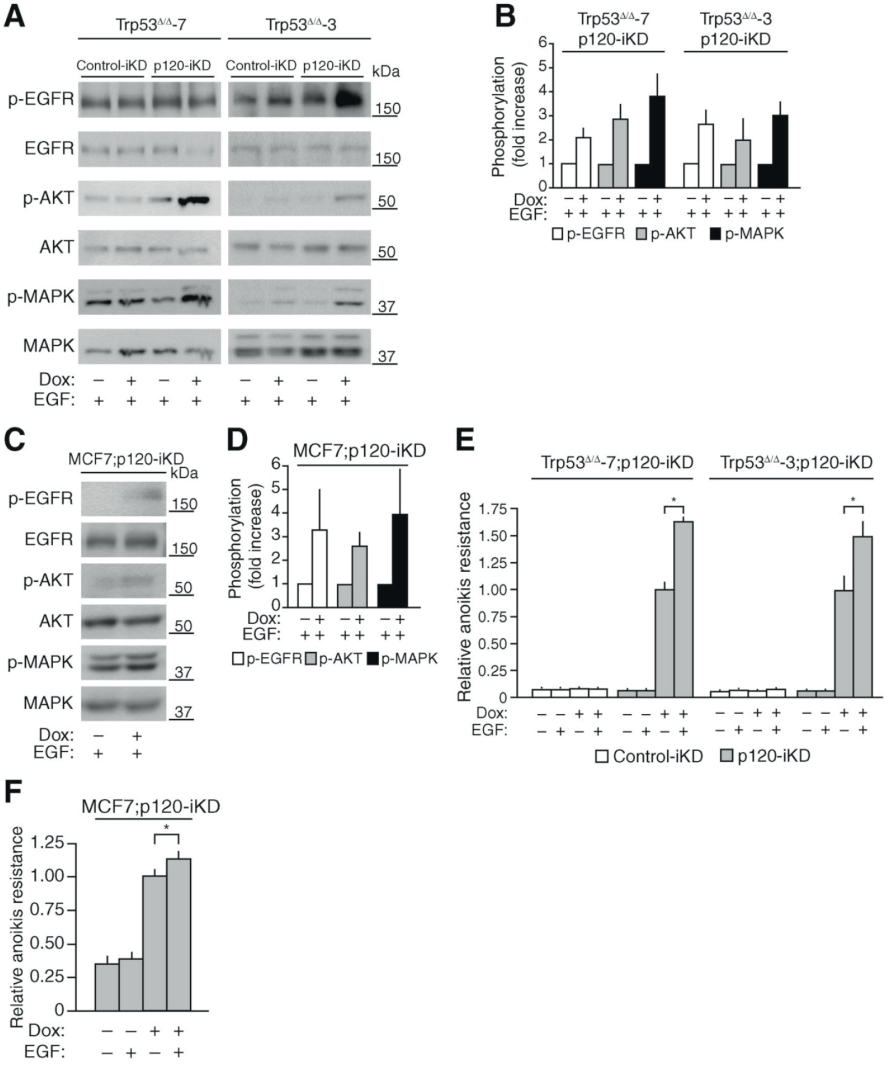

Figure 4. Loss of p120 sensitizes cells to GFR-mediated anoikis resistance. A and B, p120 knockdown sensitizes EGF signaling. Two independent Trp53$^{\Delta/\Delta}$ cell lines expressing control-iKD or p120-iKD constructs were treated with doxycycline (Dox) for 4 days, serum starved, stimulated with EGF, and subjected to Western blot analysis using phospho-specific antibodies against EGFR (top), AKT (middle), and MAPK (bottom). Total EGFR, AKT, and MAPK were used as loading controls. Quantification is shown in B. C and D, doxycycline-treated, serum-starved MCF7;p120-iKD cells were stimulated with EGF and analyzed as in A. Quantification is shown in D. E, EGF promotes anchorage-independent survival upon p120 loss. Anoikis resistance was analyzed in Trp53$^{\Delta/\Delta}$;p120-iKD cells in the presence or absence of EGF and doxycycline as indicated. Error bars represent the SD of triplicate experiments. F, EGF promotes anchorage-independent survival upon p120 loss in human breast cancer cells. Anoikis resistance of MCF7;p120-iKD cells was assayed in the presence or absence of doxycycline and EGF as indicated. *, $P < 0.05$. Error bars in B and D represent SEM of at least triplicate experiments. Error bars in E and F represent the SD of triplicate experiments.

GFR sensitization stimulates anchorage-independent viability

Because knockdown of p120 resulted in increased growth factor sensitization of pathways implicated in growth and survival, we used EGF stimulation to examine whether this mechanism could increase anchorage-independent growth and survival of breast cancer cells. We therefore plated Trp53$^{\Delta/\Delta}$;p120-iKD and Ctnnd1$^{\Delta/\Delta}$;Trp53$^{\Delta/\Delta}$ cells under anchorage-independent conditions and assayed anoikis resistance. In control cells, EGF stimulation did not mediate survival. However, addition of EGF led to an additional increase in anoikis resistance upon knockdown of p120 (Fig. 4E) and in Ctnnd1$^{\Delta/\Delta}$;Trp53$^{\Delta/\Delta}$ cell lines (Supplementary Fig. S6B). Although less prominent, EGF stimulation also induced a significant increase in anoikis resistance of MCF7;p120-iKD cells (Fig. 4F). Because adherens junction–dependent relieve of GFR inhibition is not specific for a given receptor and MCF7 responds more prominent to HGF than EGF, we also stimulated MCF7;p120-iKD cells with HGF. In line with the EGF-dependent findings in our mouse cell lines, we observed that activation of the MET receptor induced a prominent p120-dependent increase in anoikis resistance of MCF7 (Supplementary Fig. S4E).

In conclusion, we find that loss of p120 enhances anoikis resistance through increased sensitization of GFR signaling pathways, a mechanism that may stimulate metastasis in p120-negative breast cancer.

Loss of p120 leads to a proinvasive microenvironment

On the basis of the prominent presence of stroma in the metaplastic p120 null mammary carcinomas and our finding that loss of p120 induces sensitization of GFR signaling, we examined a potential source of growth factors in metastatic tumors from *Wcre;Ctnnd1$^{F/F}$;Trp53$^{F/F}$* female mice. IHC indeed revealed an abundant presence of vimentin-expressing cells surrounding p120-negative tumor cells (Fig. 5A, middle). We next analyzed p120-negative carcinomas for influx of macrophages, a renowned source of EGF (37). p120-Negative tumors from mouse and human samples contained a large macrophage-dense microenvironment (Fig. 5A and B). Moreover, a combination of IHC and RNA *in situ* hybridization revealed that the tumor-associated macrophages expressed EGF mRNA (Fig. 5C), indicating that a paracrine source of EGF is present in the tumor microenvironment.

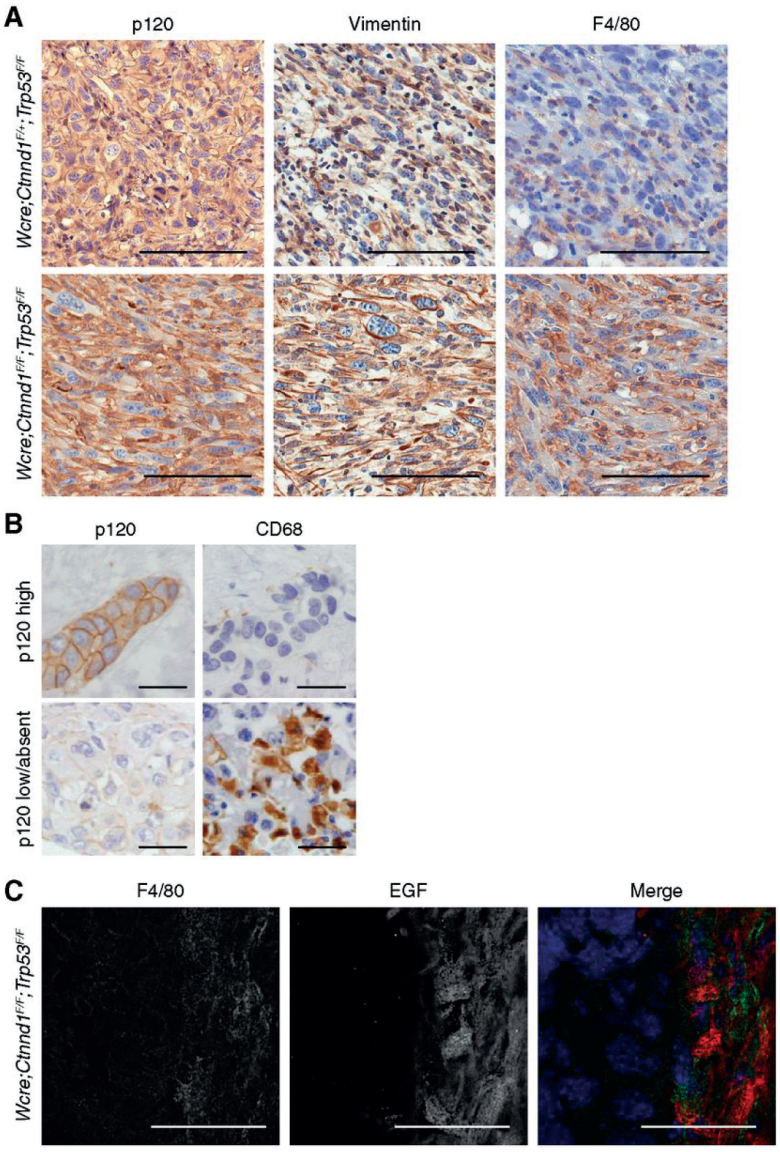

Figure 5. Loss of p120 induces cytokine production and leads to the development of a prometastatic tumor microenvironment. A, p120-deficient mammary tumors are characterized by an abundant tumor microenvironment. The presence of stromal cells/macrophages in *Wcre;Ctnnd1$^{F/+}$;Trp53$^{F/F}$* (top) and *Wcre;Ctnnd1$^{F/F}$;Trp53$^{F/F}$* (bottom) mouse mammary carcinomas were analyzed by IHC. Shown are representative stainings for p120, vimentin, and F4/80. Bars, 100 µm. B, human IDC samples were stained for p120 (left) and CD68 (macrophage marker; right). Shown are representative examples of IDC expressing high p120 (top) and low/absent p120 expression (bottom). Bars, 20 µm. C, tumor-associated macrophages produce EGF. *Wcre;Ctnnd1$^{F/F}$;Trp53$^{F/F}$* tumors were stained for macrophages using immunofluorescence (green; left) and EGF mRNA using RNA *in situ* hybridization (red; middle). DNA was visualized using 4′,6-diamidino-2-phenylindole (DAPI; blue; right). Bars, 20 µm.

In the gastrointestinal tract and skin, conditional p120 loss resulted in cytokine secretion and subsequent attraction of immune cells (18, 20, 21). To determine whether p120 loss would also control production of inflammatory cytokines in breast cancer, we assayed culture supernatant from Trp53$^{\Delta/\Delta}$;p120-iKD, Ctnnd1$^{\Delta/\Delta}$;Trp53$^{\Delta/\Delta}$, and control Trp53$^{\Delta/\Delta}$ cells using an antibody-based cytokine array. Using these tools, we observed that loss of p120 indeed increased secretion of numerous cytokines. Several of these factors are responsible for macrophage and lymphocyte attraction/maturation and stimulation of cancer-associated fibroblasts such as IL-1α (*IL1A*; ref. 38), IL-11 (*IL11*; ref. 39), and IL-12 (*IL12A*; ref. 40; Supplementary Table S4). These results suggest that p120-negative tumor cells are a paracrine source for the influx of inflammatory cells and subsequent formation of a prometastatic microenvironment.

In conclusion, we show that loss of p120 results in the excretion of cytokines that may control influx of macrophages and other stromal cells that can promote progression of p120-negative tumor cells through the induction of sensitized GFRs signaling pathways.

DISCUSSION

p120 Loss leads to anoikis resistance and metastasis

In breast cancer, disruption of adherens junction complex formation through early mutational inactivation of E-cadherin leads to the development of ILC (3–5). Upon inactivation of E-cadherin, p120 translocates to the cytosol, where it functions as an oncogene controlling Rock-mediated anoikis resistance of ILC cells (8). In contrast to ILC, most IDC cases retain expression of a functional adherens junction complex that may be inactivated through epigenetic mechanisms at later stages of breast cancer progression (6). Interestingly, and in contrast to the salivary gland (17), gastrointestinal tract (20, 21), dental enamel (16), ocular tissue (19), and skin (18), somatic inactivation of p120 in the mammary gland is not tolerated (15). These tissue-specific differences are further exemplified by the fact that conditional p120 ablation in the upper gastrointestinal tract resulted in the formation of invasive squamous esophageal carcinomas (21).

To determine a possible role for p120 during breast cancer progression, we crossed the conditional p120 allele (41) onto the *Wcre;Trp53*$^{F/F}$ mouse model of noninvasive breast cancer. Using this compound mouse model, we observed that—whereas onset and incidence of primary tumor development were unaffected—homozygous p120 loss resulted in metastatic disease. Interestingly, metastatic spread was not reported in other conditional p120 tumor models (17, 18, 20). Metastatic spread of tumors

from *Wcre;Trp53$^{F/F}$* and *Wcre;Ctnnd1$^{F/+}$;Trp53$^{F/F}$* female mice was a rare event. Because E-cadherin remained expressed and derivate cell lines functionally displayed anchorage dependence, it indicated that E-cadherin expression is the rate-limiting factor preventing initial tumor cell invasion and metastasis upon p120 loss. Supporting this assumption is our observation that E-cadherin is temporally retained on the cell surface upon p120 inactivation in preinvasive CIS-type lesions from *Wcre;Ctnnd1$^{F/F}$;Trp53$^{F/F}$* mice. Also, we have shown previously that low E-cadherin expression levels are sufficient to induce anchorage dependency in anoikis-resistant mouse ILC (mILC) cells (4, 5).

Interestingly, and in contrast to mutational E-cadherin loss, we observed that somatic p120 inactivation did not result in the formation of ILC, but instead resulted in metaplastic carcinoma. Differences may be explained by the fact that p120 plays a key oncogenic role in ILC progression through myosin phosphatase Rho interacting protein-dependent regulation of the Rho, Rock, and the cytoskeleton (8, 42). Moreover, in contrast to E-cadherin inactivation, we did not observe metastases in typical ILC dissemination sites such as bone marrow and gastrointestinal tract in the current p120 conditional knockout model. Finally, dual inactivation of p120 and p53 did not accelerate tumor development as seen for combined E-cadherin and p53 loss (4, 5). These phenotypic and functional differences between p120 and E-cadherin suggest that although the overall consequence is adherens junction inactivation and metastasis, p120 loss leads to a biochemically and functionally different breast cancer phenotype.

p120 Loss sensitizes cells to GFR signaling

How does p120 loss regulate anoikis resistance? Our data indicate that p120 loss results in a decrease of E-cadherin–dependent proapoptotic signals in the absence of anchorage, resulting in anoikis. In this scenario, heterozygous p120 loss will not result in metastasis, because residual membranous E-cadherin expression will lead to anoikis in cells that escape from the primary tumor. An additional scenario may be provided by GFR signaling. Membrane receptors can directly influence the activity of unrelated neighboring receptors (43). Depending on cellular context, E-cadherin expression may influence EGFR activation (35, 36). Indeed, studies in gastric cancer showed that germline and somatic (in-frame deleterious) mutations in the E-cadherin extracellular domain lead to increased activation of EGFR signaling (44). We show here that inactivation of the adherens junction through loss of p120 leads to increased sensitization of GFR signaling, a phenomenon that is likely dependent on E-cadherin turnover. Although it is still controversial whether this mechanism is ligand dependent, our data indicate that the GFR hypersensitivity upon p120 loss is not caused by upregulation of EGFR expression

levels or increased EGF binding at the cell surface (Fig. 4A and Supplementary Fig. S5C). Given our observation that E-cadherin–dependent inhibition of GFR signaling is not specific for a given receptor, it seems unlikely that specific posttranslational modifications or a specific phosphatase/kinase regulates this process.

A possible scenario may therefore be that E-cadherin elicits a general inhibitory effect on the recruitment of proximal activating molecules and docking adaptors such as Gab1 (*GAB1*), Grb2 (*GRB2*), or Sos (*SOS1*) to sites of tyrosine kinase phosphorylation (45, 46), resulting in a dampening of pathway activation downstream of the GFR. Alternatively, the extracellular domain of E-cadherin could play a role in preventing activation of EGFR, because shedding of E-cadherin has been implicated in EGF-dependent activation of the PI3K/AKT and MAPK pathways and subsequent cell survival (47). Thus, although further research is needed to delineate the exact mechanism that controls the sensitization of GFR signaling upon p120 loss, we propose that increased sensitization of GFR signaling may be caused by a relieve of direct or indirect mechanical restriction, or inhibition of ligand binding as a result of steric hindrance between the adherens junction and GFRs.

Loss of p120 results in a prometastatic microenvironment

Although the precise nature of the influx of inflammatory cells may depend on the model system studied, several groups reported that p120 ablation may lead to inflammation (18, 20, 21). In line with this, we found that loss of p120 results in the development of stromal dense and macrophage-rich mammary tumors. Furthermore, we show that loss of p120 leads to secretion of several cytokines, which may control the recruitment of inflammatory cells (e.g., macrophages) that have been implicated in inflammation-associated cancer initiation and promotion (48) and are correlated with poor prognosis in breast cancer (49, 50). Moreover, it has been well established that mammary tumor cells may instigate a paracrine loop that involves the production of chemoattractants and subsequent recruitment of EGF-producing macrophages, resulting in activation of prometastatic pathways in tumor cells (51, 52).

In closing, we propose that p120 inactivation and subsequent E-cadherin loss is a late event in IDC tumor progression. To our knowledge, there have been no reports on mutational p120 inactivation in breast cancer. Although such mutations could have easily been missed using past sequencing techniques and the fact that p120 loss is often observed in only a small percentage of the tumor, *CTNND1* mutations are most probably a rare event. Conversely, this could also indicate that p120 inactivation in IDC may be caused by epigenetic or other indirect mechanisms, as has been shown for E-cadherin

(53–55). This, and because of the fact that homozygous p120 inactivation in mice does not induce the formation of mILC, leads us to hypothesize that inactivation of p120 probably occurs during late progression of invasive breast cancer. Although the exact mechanism that regulates p120 inactivation remains to be resolved, our data show that E-cadherin–dependent inhibition of GFR signaling is relieved upon inactivation of p120. As a consequence, anoikis-resistant cells are sensitized to prometastatic growth factors. Because others and we show that p120 loss also facilitates concomitant formation of a prometastatic microenvironment, inactivation of p120 induces multiple hallmarks of metastatic cancer. A simplified model of our findings is presented in Fig. 6.

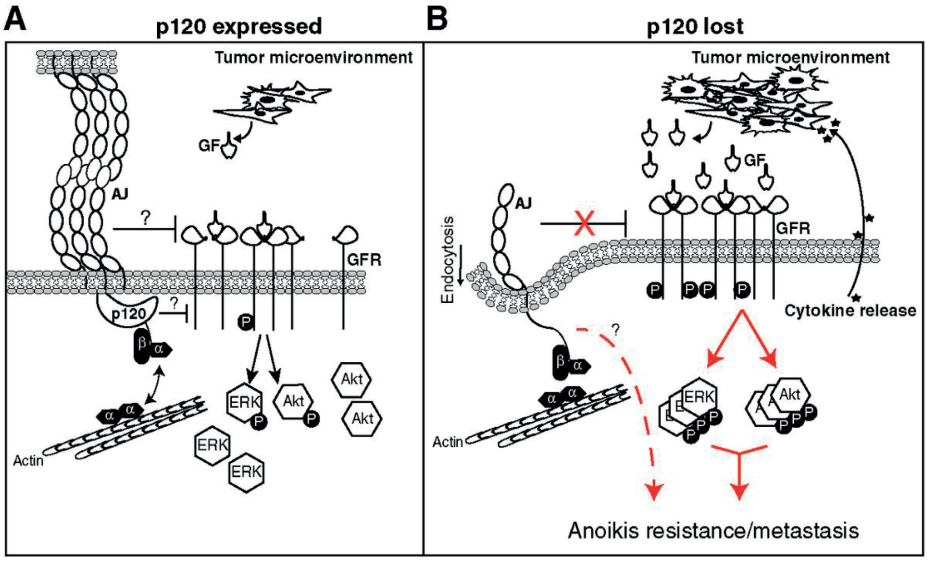

Figure 6. A model for p120 as a breast cancer metastasis suppressor. A, in the presence of p120, E-cadherin is stabilized at the plasma membrane leading to the formation of adherens junctions. The adherens junction inhibits growth factor (GF)–induced GFR activation through currently unknown mechanisms. B, upon loss of p120 the adherens junction is dismantled and E-cadherin and β-catenin are degraded. As a result, anoikis resistance is induced, and subsequently enhanced by hypersensitized GFR signaling due to the relief of E-cadherin–dependent GFR inhibition. In addition, loss of p120 induces cytokine secretion, resulting in stimulation of the tumor microenvironment. This may facilitate a paracrine loop that activates sensitized GFR signaling in p120-negative tumor cells. The exact mechanism behind this increased sensitization is currently unknown, but does not seem to involve increased GFR expression, autocrine GFR activation, or increased growth factor binding. ERK, extracellular signal–regulated kinase.

We think that our findings may have substantial clinical ramifications. In our model, GFR signaling can be enhanced independent of GFR expression levels. Thus, our data imply that the mere presence of certain GFRs is of clinical importance, provided

that breast cancer cells are p120 negative. Accordingly and depending on the GFRs expressed, patients suffering from p120-negative IDC may be eligible for treatment with GFR inhibitors targeting the expressed receptors. We have thus uncovered a tumor-promoting role for p120 in breast cancer progression that provides an alternate rationale for therapeutic intervention of p120-negative metastatic breast cancer.

DISCLOSURE OF POTENTIAL CONFLICTS OF INTEREST

No potential conflicts of interest were disclosed.

AUTHORS' CONTRIBUTIONS

Conception and design: R.C.J. Schackmann, J. Jonkers, P.W.B. Derksen

Development of methodology: R.C.J. Schackmann, T. Peeters, P.J. van Diest, P.W.B. Derksen

Acquisition of data (provided animals, acquired and managed patients, provided facilities, etc.): R.C.J. Schackmann, S. Klarenbeek, E.J. Vlug, S. Stelloo, M. Tenhagen, J.F. Vermeulen, P.J. van Diest, J. Jonkers

Analysis and interpretation of data (e.g., statistical analysis, biostatistics, computational analysis): R.C.J. Schackmann, S. Klarenbeek, S. Stelloo, J.F. Vermeulen, P.J. van Diest, J. Jonkers, P.W.B. Derksen

Writing, review, and/or revision of the manuscript: R.C.J. Schackmann, S. Klarenbeek, J.F. Vermeulen, E. van der Wall, P.J. van Diest, J. Jonkers, P.W.B. Derksen

Administrative, technical, or material support (i.e., reporting or organizing data, constructing databases): S. Klarenbeek, M. van Amersfoort, M. Tenhagen, T.M. Braumuller, P. van der Groep, P.W.B. Derksen

Study supervision: J. Jonkers, P.W.B. Derksen

GRANT SUPPORT

This work was supported by the UMC Cancer Center and grants from the Netherlands Organization for Scientific Research (NWO-VIDI 917.96.318) and the Dutch Cancer Society (UU-KWF 2011 5230).

The costs of publication of this article were defrayed in part by the payment of page charges. This article must therefore be hereby marked *advertisement* in accordance with 18 U.S.C. Section 1734 solely to indicate this fact.

ACKNOWLEDGMENTS

The authors thank Eva Schut-Kregel for excellent technical support, Juliet Daniel for providing the p120-1A cDNA and Al Reynolds for the p120 conditional mice. Participants of the MMM meeting and members of the Bos, Burgering, and Pathology labs are acknowledged for help and fruitful discussions. The authors also thank the University Medical Center (UMC) Biobank.

REFERENCES

1. Pokutta S, Weis WI. Structure and mechanism of cadherins and catenins in cell–cell contacts. Annu Rev Cell Dev Biol 2007;23:237–61.
2. Jeanes A, Gottardi CJ, Yap AS. Cadherins and cancer: how does cadherin dysfunction promote tumor progression? Oncogene 2008; 27:6920–9.
3. Berx G, Cleton-Jansen AM, Nollet F, de Leeuw WJ, van de Vijver M, Cornelisse C, et al. E-cadherin is a tumour/invasion suppressor gene mutated in human lobular breast cancers. EMBO J 1995;14: 6107–15.
4. Derksen PW, Braumuller TM, van der Burg E, Hornsveld M, Mesman E, Wesseling J, et al. Mammary-specific inactivation of E-cadherin and p53 impairs functional gland development and leads to pleomorphic invasive lobular carcinoma in mice. Dis Model Mech 2011; 4:347–58.
5. Derksen PW, Liu X, Saridin F, van der Gulden H, Zevenhoven J, Evers B, et al. Somatic inactivation of E-cadherin and p53 in mice leads to metastatic lobular mammary carcinoma through induction of anoikis resistance and angiogenesis. Cancer Cell 2006;10:437–49.
6. Gould Rothberg BE, Bracken MB. E-cadherin immunohistochemical expression as a prognostic factor in infiltrating ductal carcinoma of the breast: a systematic review and meta-analysis. Breast Cancer Res Treat 2006;100:139–48.
7. Kalluri R, Weinberg RA. The basics of epithelial–mesenchymal transition. J Clin Invest 2009;119:1420–8.
8. Schackmann RC, van Amersfoort M, Haarhuis JH, Vlug EJ, Halim VA, Roodhart JM, et al. Cytosolic p120-catenin regulates growth of metastatic lobular carcinoma through Rock1-mediated anoikis resistance. J Clin Invest 2011;121:3176–88.
9. Soto E, Yanagisawa M, Marlow LA, Copland JA, Perez EA, Anastasiadis PZ. p120 catenin induces opposing effects on tumor cell growth depending on E-cadherin expression. J Cell Biol 2008;183:737–49.
10. Reynolds AB, Daniel J, McCrea PD, Wheelock MJ, Wu J, Zhang Z. Identification of a new catenin: the tyrosine kinase substrate p120cas associates with E-cadherin complexes. Mol Cell Biol 1994;14:8333–42.
11. Fujita Y, Krause G, Scheffner M, Zechner D, Leddy HE, Behrens J, et al. Hakai, a c-Cbl-like protein, ubiquitinates and induces endocytosis of the E-cadherin complex. Nat Cell Biol 2002;4:222–31.
12. Baki L, Marambaud P, Efthimiopoulos S, Georgakopoulos A, Wen P, Cui W, et al. Presenilin-1 binds cytoplasmic epithelial cadherin, inhibits cadherin/p120 association, and regulates stability and function of the cadherin/catenin adhesion complex. Proc Natl Acad Sci U S A 2001;98:2381–6.
13. Sato K, Watanabe T, Wang S, Kakeno M, Matsuzawa K, Matsui T, et al. Numb controls E-cadherin endocytosis through p120 catenin with aPKC. Mol Biol Cell 2011;22:3103–19.
14. Boussadia O, Kutsch S, Hierholzer A, Delmas V, Kemler R. E-cadherin is a survival factor for the lactating mouse mammary gland. Mech Dev 2002;115:53–62.

15. Kurley SJ, Bierie B, Carnahan RH, Lobdell NA, Davis MA, Hofmann I, et al. p120-catenin is essential for terminal end bud function and mammary morphogenesis. Development 2012;139:1754–64.
16. Bartlett JD, Dobeck JM, Tye CE, Perez-Moreno M, Stokes N, Reynolds AB, et al. Targeted p120-catenin ablation disrupts dental enamel development. PLoS ONE 2010;5:e12703.
17. Davis MA, Reynolds AB. Blocked acinar development, E-cadherin reduction, and intraepithelial neoplasia upon ablation of p120-catenin in the mouse salivary gland. Dev Cell 2006;10:21–31.
18. Perez-Moreno M, Davis MA, Wong E, Pasolli HA, Reynolds AB, Fuchs E. p120-catenin mediates inflammatory responses in the skin. Cell 2006;124:631–44.
19. Tian H, Sanders E, Reynolds A, van Roy F, van Hengel J. Ocular anterior segment dysgenesis upon ablation of p120 catenin in neural crest cells. Invest Ophthalmol Vis Sci 2012;53:5139–53.
20. Smalley-Freed WG, Efimov A, Burnett PE, Short SP, Davis MA, Gumucio DL, et al. p120-catenin is essential for maintenance of barrier function and intestinal homeostasis in mice. J Clin Invest 2010;120:1824–35.
21. Stairs DB, Bayne LJ, Rhoades B, Vega ME, Waldron TJ, Kalabis J, et al. Deletion of p120-catenin results in a tumor microenvironment with inflammation and cancer that establishes it as a tumor suppressor gene. Cancer Cell 2011;19:470–83.
22. Dillon DA, D'Aquila T, Reynolds AB, Fearon ER, Rimm DL. The expression of p120ctn protein in breast cancer is independent of alpha- and beta-catenin and E-cadherin.AmJ Pathol 1998;152:75–82.
23. Nakopoulou L, Gakiopoulou-Givalou H, Karayiannakis AJ, Giannopoulou I, Keramopoulos A, Davaris P, et al. Abnormal alpha-catenin expression in invasive breast cancer correlates with poor patient survival. Histopathology 2002;40:536–46.
24. Talvinen K, Tuikkala J, Nykanen M, Nieminen A, Anttinen J, Nevalainen OS, et al. Altered expression of p120catenin predicts poor outcome in invasive breast cancer. J Cancer Res Clin Oncol 2010;136:1377–87.
25. Dull T, Zufferey R, Kelly M, Mandel RJ, Nguyen M, Trono D, et al. A third-generation lentivirus vector with a conditional packaging system. J Virol 1998;72:8463–71.
26. Reid T, Furuyashiki T, Ishizaki T, Watanabe G, Watanabe N, Fujisawa K, et al. Rhotekin, a new putative target for Rho bearing homology to a serine/threonine kinase, PKN, and rhophilin in the rho-binding domain. J Biol Chem 1996;271:13556–60.
27. Derksen PW, Tjin E, Meijer HP, Klok MD, MacGillavry HD, van Oers MH, et al. Illegitimate WNT signaling promotes proliferation of multiple myeloma cells. Proc Natl Acad Sci U S A 2004;101:6122–7.
28. Vermeulen JF, van de Ven RA, Ercan C, van der Groep P, van der Wall E, Bult P, et al. Nuclear Kaiso expression is associated with high grade and triple-negative invasive breast cancer. PLoS ONE 2012;7:e37864.
29. Birchmeier W, Hulsken J, Behrens J. E-cadherin as an invasion suppressor. Ciba Found Symp 1995;189:124–36.
30. Luini A, Aguilar M, Gatti G, Fasani R, Botteri E, Brito JA, et al. Metaplastic carcinoma of the breast, an unusual disease with worse prognosis: the experience of the European Institute of Oncology and review of the literature. Breast Cancer Res Treat 2007;101:349–53.

31. Douma S, Van Laar T, Zevenhoven J, Meuwissen R, Van Garderen E, Peeper DS. Suppression of anoikis and induction of metastasis by the neurotrophic receptor TrkB. Nature 2004;430:1034–9.
32. Liu Y, Xu HT, Dai SD, Wei Q, Yuan XM, Wang EH. Reduction of p120 (ctn) isoforms 1 and 3 is significantly associated with metastatic progression of human lung cancer. APMIS 2007;115:848–56.
33. Hanahan D, Weinberg RA. Hallmarks of cancer: the next generation. Cell 2011;144:646–74.
34. Takahashi K, Suzuki K. Density-dependent inhibition of growth involves prevention of EGF receptor activation by E-cadherin-mediated cell-cell adhesion. Exp Cell Res 1996;226:214–22.
35. Qian X, Karpova T, Sheppard AM, McNally J, Lowy DR. E-cadherin-mediated adhesion inhibits ligand-dependent activation of diverse receptor tyrosine kinases. EMBO J 2004;23:1739–48.
36. Reddy P, Liu L, Ren C, Lindgren P,Boman K, Shen Y, et al. Formation of E-cadherin-mediated cell-cell adhesion activates AKT and mitogen activated protein kinase via phosphatidylinositol 3 kinase and ligandindependent activation of epidermal growth factor receptor in ovarian cancer cells. Mol Endocrinol 2005;19:2564–78.
37. Pollard JW. Macrophages define the invasive microenvironment in breast cancer. J Leukoc Biol 2008;84:623–30.
38. Nozaki S, Sledge GW Jr, Nakshatri H. Cancer cell-derived interleukin 1alpha contributes to autocrine and paracrine induction of pro-metastatic genes in breast cancer. Biochem Biophys Res Commun 2000; 275:60–2.
39. Musashi M, Clark SC, Sudo T, Urdal DL, Ogawa M. Synergistic interactions between interleukin-11 and interleukin-4 in support of proliferation of primitive hematopoietic progenitors of mice. Blood 1991;78:1448–51.
40. Trinchieri G. Interleukin-12: a cytokine at the interface of inflammation and immunity. Adv Immunol 1998;70:83–243.
41. Davis MA, Ireton RC, Reynolds AB. A core function for p120-catenin in cadherin turnover. J Cell Biol 2003;163:525–34.
42. Shibata T, Kokubu A, Sekine S, Kanai Y, Hirohashi S. Cytoplasmic p120ctn regulates the invasive phenotypes of E-cadherin-deficient breast cancer. Am J Pathol 2004;164:2269–78.
43. Chen X, Gumbiner BM. Crosstalk between different adhesion molecules. Curr Opin Cell Biol 2006;18:572–8.
44. Bremm A, Walch A, Fuchs M, Mages J, Duyster J, Keller G, et al. Enhanced activation of epidermal growth factor receptor caused by tumor-derived E-cadherin mutations. Cancer Res 2008;68:707–14.
45. Holgado-Madruga M, Emlet DR, MoscatelloDK, Godwin AK,WongAJ. A Grb2-associated docking protein in EGF- and insulin-receptor signalling. Nature 1996;379:560–4.
46. Yamasaki S, Nishida K, Yoshida Y, Itoh M, Hibi M, Hirano T. Gab1 is required for EGF receptor signaling and the transformation by activated ErbB2. Oncogene 2003;22:1546–56.
47. Inge LJ, Barwe SP, D'Ambrosio J, Gopal J, Lu K, Ryazantsev S, et al. Soluble E-cadherin promotes cell survival by activating epidermal growth factor receptor. Exp Cell Res 2011;317:838–48.

48. Balkwill F, Charles KA, Mantovani A. Smoldering and polarized inflammation in the initiation and promotion of malignant disease. Cancer Cell 2005;7:211–7.
49. Murri AM, Hilmy M, Bell J, Wilson C, McNicol AM, Lannigan A, et al. The relationship between the systemic inflammatory response, tumour proliferative activity, T-lymphocytic and macrophage infiltration, microvessel density and survival in patients with primary operable breast cancer. Br J Cancer 2008;99:1013–9.
50. Ueno T, Toi M, Saji H, Muta M, Bando H, Kuroi K, et al. Significance of macrophage chemoattractant protein-1 in macrophage recruitment, angiogenesis, and survival in human breast cancer. Clin Cancer Res 2000;6:3282–9.
51. Condeelis J, Pollard JW. Macrophages: obligate partners for tumor cell migration, invasion, and metastasis. Cell 2006;124:263–6.
52. Qian BZ, Pollard JW. Macrophage diversity enhances tumor progression and metastasis. Cell 2010;141:39–51.
53. Batlle E, Sancho E, Franci C, Dominguez D, Monfar M, Baulida J, et al. The transcription factor snail is a repressor of E-cadherin gene expression in epithelial tumour cells. Nat Cell Biol 2000;2:84–9.
54. Graff JR, Herman JG, Lapidus RG, Chopra H, Xu R, Jarrard DF, et al. Ecadherin expression is silenced by DNA hypermethylation in human breast and prostate carcinomas. Cancer Res 1995;55:5195–9.
55. Hajra KM, Chen DY, Fearon ER. The SLUG zinc-finger protein represses E-cadherin in breast cancer. Cancer Res 2002;62: 1613–8.

SUPPLEMENTAL FIGURES

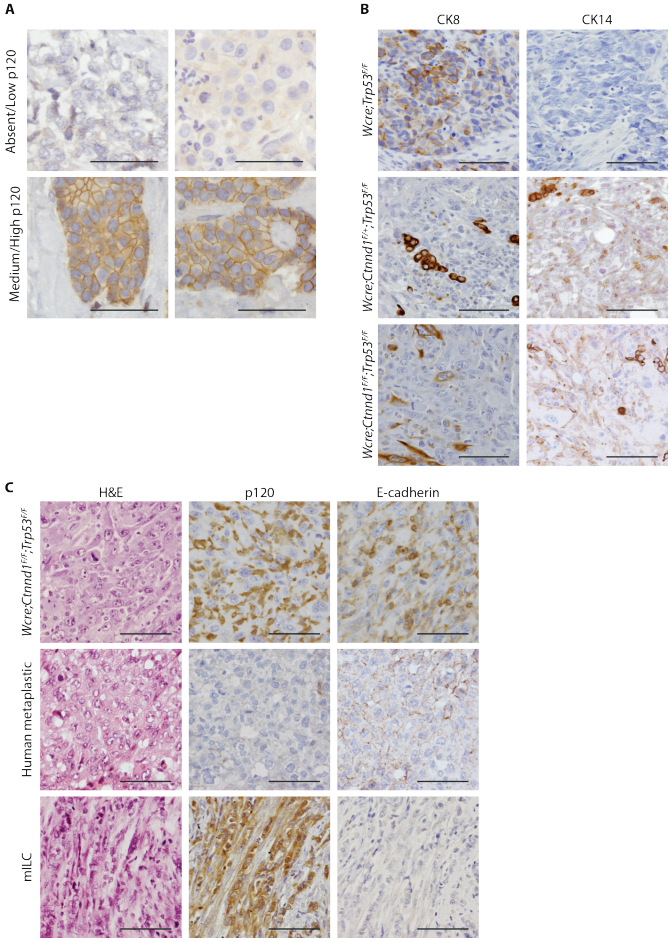

Figure S1

Comparative immunohistochemistry in human and mouse breast cancer. **A)** p120 expression in human IDC. A panel of 298 invasive ductal carcinomas was analyzed for p120 expression by immunohistochemistry. Depicted are four representative p120 expression patterns showing low/absent p120 expression (top panels) and medium to high expression levels (bottom panels). **B)** Epithelial cytokeratin expression in mammary carcinomas from the p120 conditional mouse model. Expression of cytokeratin (CK) 8 (left panels) and CK14 (right panels) are shown for mammary tumors that developed in, *Wcre;Trp53*$^{F/F}$ (top panels), *Wcre;Ctnnd1*$^{F/+}$*;Trp53*$^{F/F}$ (middle panels) and *Wcre;Ctnnd1*$^{F/F}$*;Trp53*$^{F/F}$ (bottom panels) conditional female mice. **C)** Loss of p120 in mouse mammary tumors leads to the development of metaplastic carcinoma. Shown are representative expression patterns of p120 and E-cadherin in mouse metaplastic carcinoma (top panels), human metaplastic carcinoma (middle panels) and mouse ILC (bottom panels). Note the absence of p120 and the punctate E-cadherin localization in the metaplastic tumors. In contrast, mouse ILC that developed in *Wcre;Ctnnd*$^{F/F}$*;Trp53*$^{F/F}$ female mice is characterized by loss of E-cadherin and subsequent cytosolic localization of p120. Bars: 50µM.

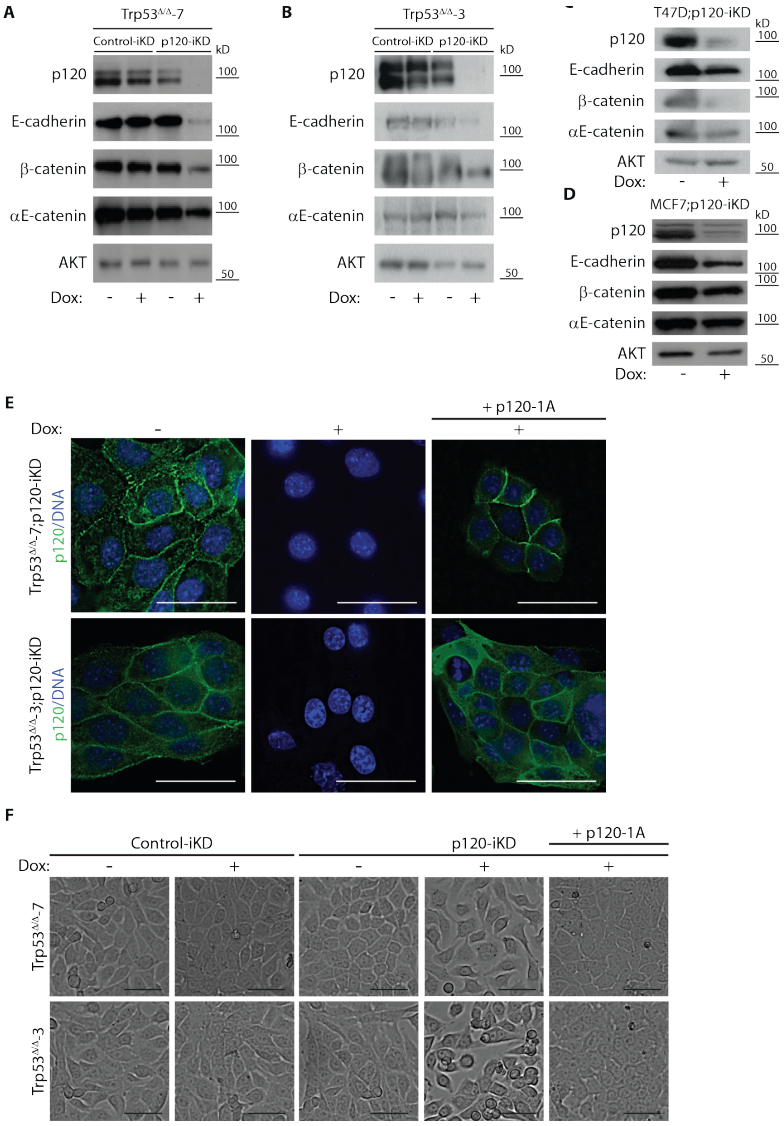

Figure S2

p120 knockdown decreases AJ member expression levels and disrupts cell-cell contact in breast cancer cells. **A-D)** Dox-treated and untreated Control-iKD and Trp53$^{\Delta/\Delta}$;p120-iKD mouse mammary carcinoma cells (A and B) and human T47D;p120-iKD (C) and MCF7;p120-iKD cells (D) were subjected to western blot analysis, showing the effect of p120 knockdown on E-cadherin, β-catenin and αEcatenin expression levels. AKT was used as loading control. **E and F**) p120 controls epithelial integrity of mammary carcinoma cells. Trp53$^{\Delta/\Delta}$;p120-iKD and Trp53$^{\Delta/\Delta}$;p120-iKD cells expressing p120-1A were stained for p120 (green) to visualize knockdown and correct relocalization. DNA was visualized using DAPI (blue). Trp53$^{\Delta/\Delta}$ cell lines expressing inducible control (Control-iKD) or Trp53$^{\Delta/\Delta}$;p120-iKD and Trp53$^{\Delta/\Delta}$;p120-iKD cells expressing p120-1A were grown in the absence or presence of Dox for 4 days. Pictures were taken using bright field microscopy to show epithelial monolayer integrity (F). Bars: 50 µm.

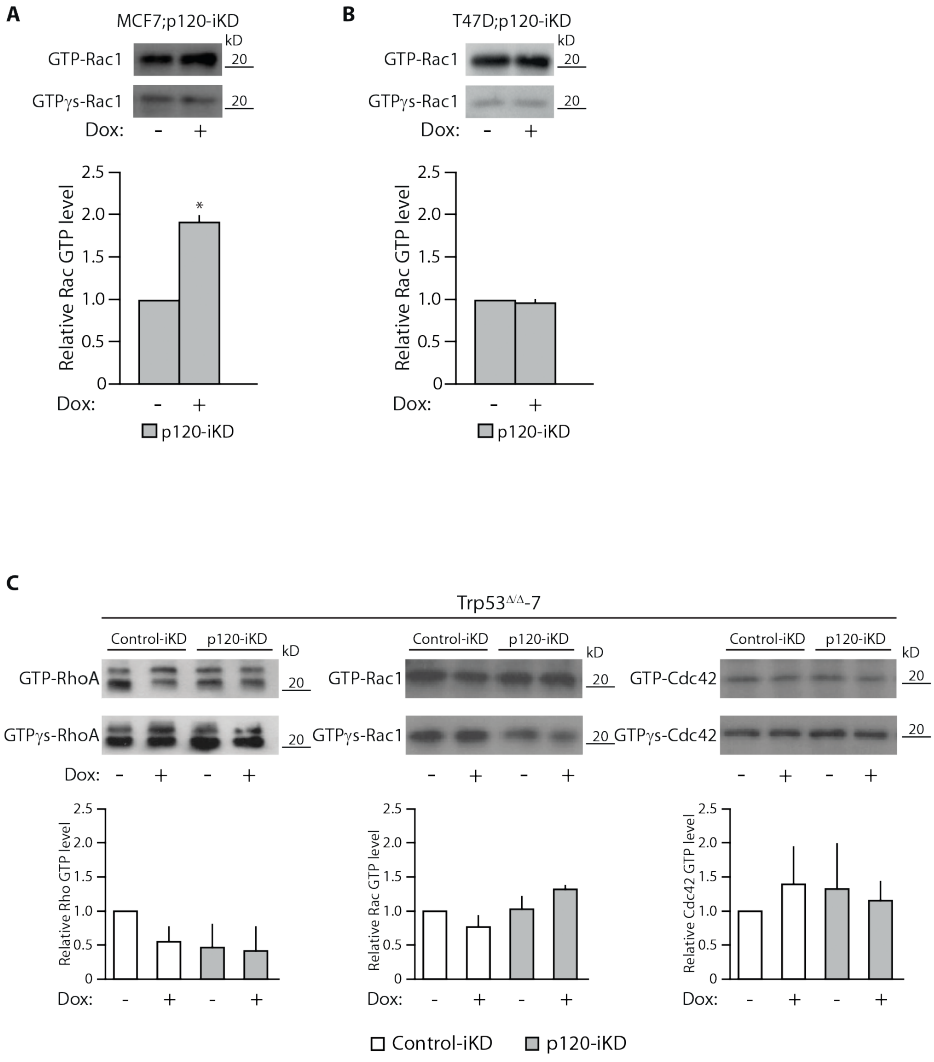

Figure S3

Loss of p120 does not affect Rho GTPase activity. **A and B)** Rac1 activity in MCF7;p120-iKD and T47D;p120-IKD cells. GTP-bound Rac1 levels were determined using pulldown assays and subsequent western blotting. Total GTPγs-bound Rac1 levels are shown as loading control. Lower graph represents the quantification of triplicate experiments. Error bars represent SD. **C)** RhoA, Rac1 and Cdc42 activity was assessed in $Trp53^{\Delta/\Delta}$;Control-iKD and p120-iKD cells after Dox treatment. Western blot analysis shows the levels of GTP-bound Rho, Rac1 and Cdc42 (upper blots) and the corresponding GTPγs-bound levels as loading controls (lower blots). Lower graphs represent the quantification of triplicate experiments, normalized against untreated Control-iKD cells. Error bars represent SD of triplicate experiments.

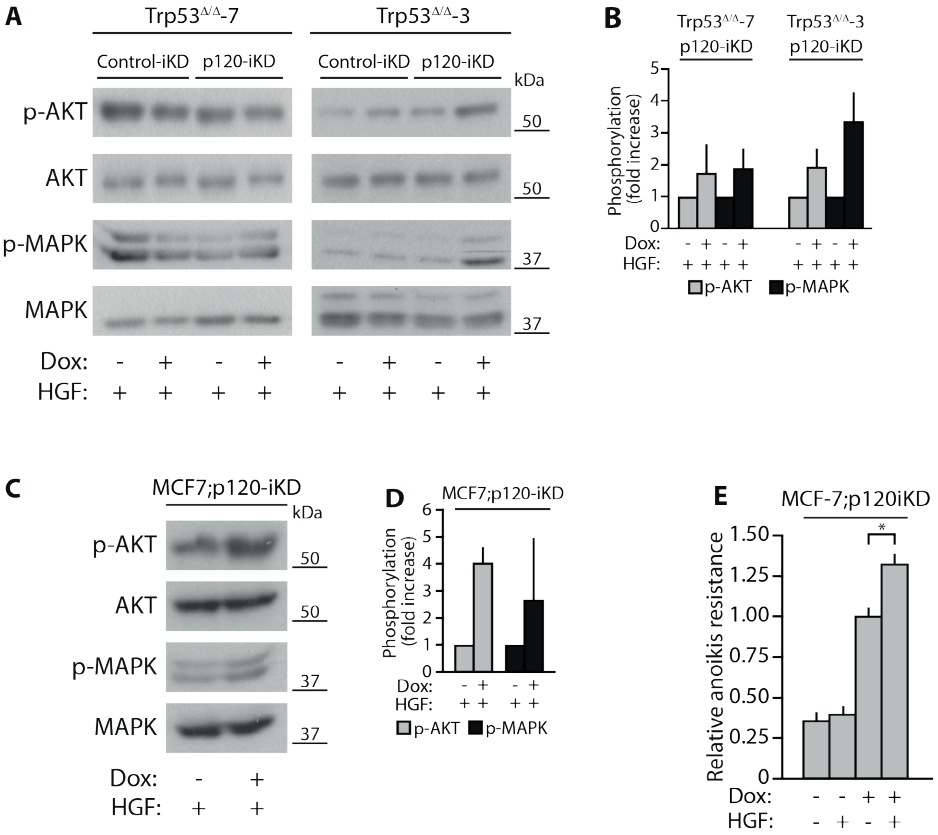

Figure S4

Loss of AJ integrity sensitizes cells to HGF signaling. **A and B)** p120 knockdown results in sensitization to HGF-induced signaling. Two independent Trp53$^{\Delta/\Delta}$ cell lines expressing Control-iKD or p120-iKD were treated with Dox for 4 days, serum starved, stimulated with HGF and subjected to western blot analysis for phosphorylated AKT and MAPK. Total AKT and MAPK were used as loading controls. Quantification is shown in (B). **C and D)** MCF7;p120-iKD cells were cultured in the presence of Dox, serum starved, stimulated with HGF and subjected to western blot analysis as in (A). Quantification is shown in (D). **E)** HGF promotes anchorage independent survival upon p120 loss in human breast cancer cells. Dox-induced MCF7;p120-iKD cells were cultured in ultra-low cluster plates for 4 days in the presence or absence of Dox and HGF as indicated. *=p<0.05. Error bars in B and D represent the standard error of the mean based on triplicate experiments. Error bars in E represent the SD of triplicate experiments.

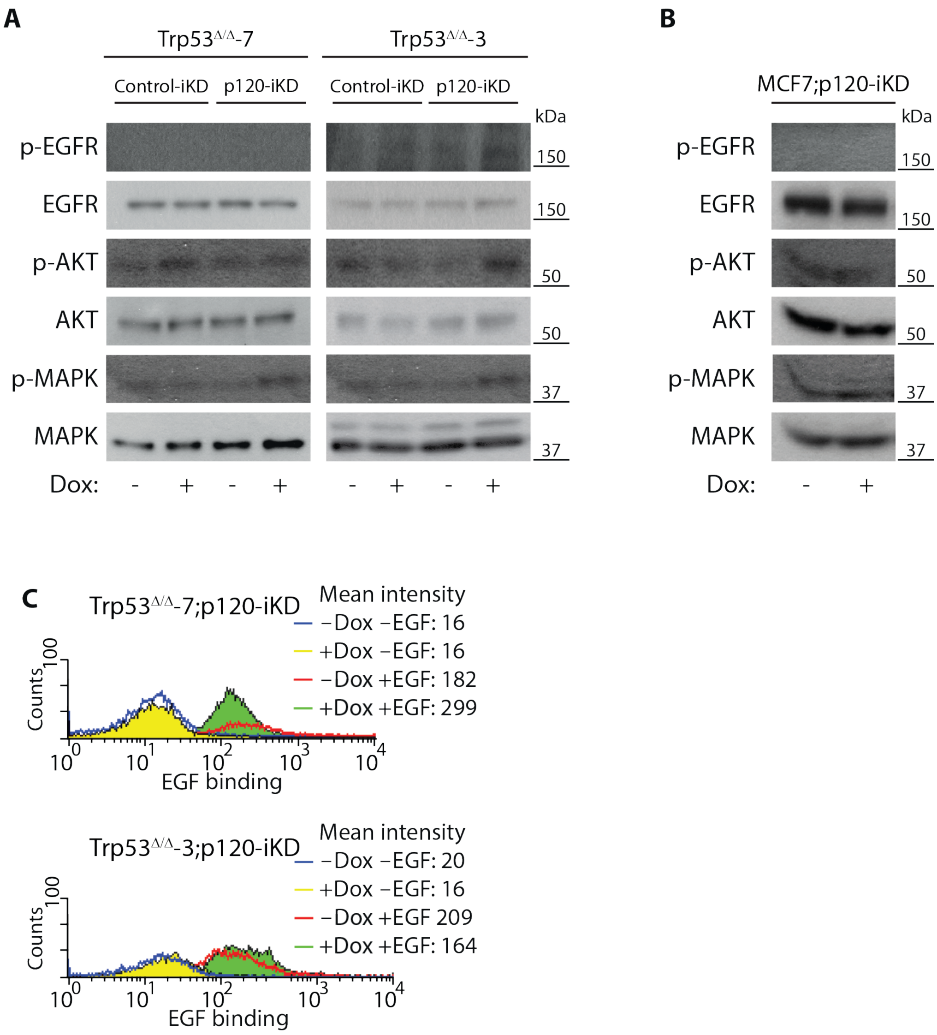

Figure S5

Loss of p120 and subsequent AJ inactivation does not induce autocrine survival pathways or increased EGF binding. **A and B)** knockdown of p120 does not activate AKT or MAPK signaling under anchorage-dependent conditions. Two independent Trp53$^{\Delta/\Delta}$ cell lines (A) and MCF7 cells (B) expressing Control-iKD or p120-iKD constructs were serum starved, and subjected to western blot analysis for phosphorylated EGFR (upper panels), AKT (middle panels) and MAPK (lower panels) (long exposure). Total EGFR, AKT and MAPK were used as loading controls. Note the near absence of phosphorylation signal upon p120 knockdown. **C)** p120 knockdown does not increase quantitative EGF-binding. p120-iKD expressing Trp53$^{\Delta/\Delta}$ cell lines were treated with Dox for 4 days, serum-starved and trypsinized. Ice-cold cells were incubated with or without Alexa647-conjugated EGF and subjected to FACS analysis.

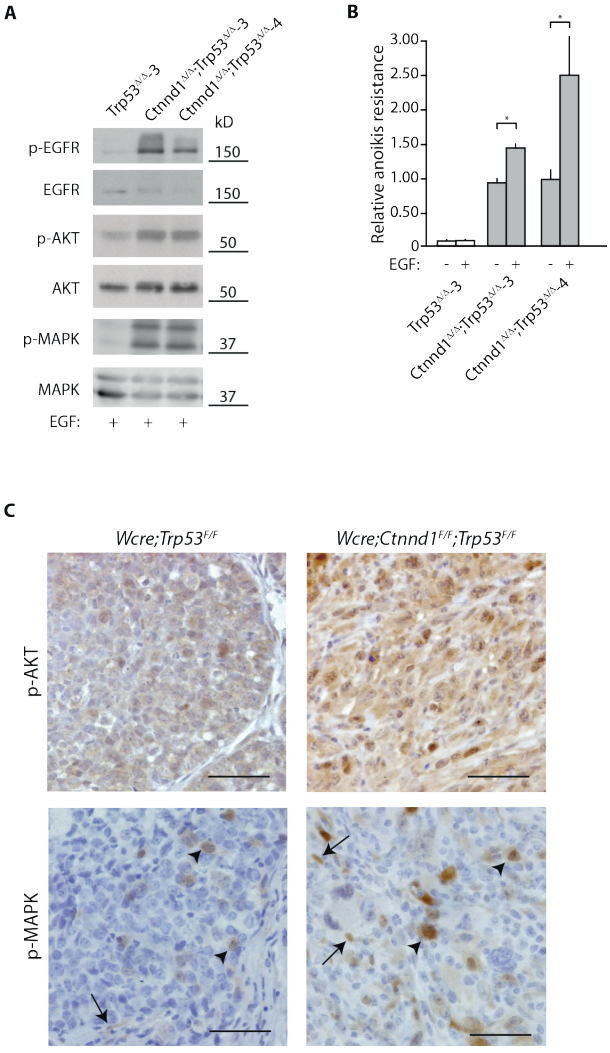

Figure S6

p120 knockout sensitizes tumor cells to growth factor signaling. **A**) Two independent p120 knockout cell lines (Ctnnd1$^{\Delta/\Delta}$;Trp53$^{\Delta/\Delta}$) were generated from tumors that developed in *Wcre;Ctnnd1$^{F/F}$;Trp53$^{F/F}$* female mice. Cells were serum starved, stimulated with EGF and subjected to western blot analysis using phospho-specific antibodies against EGFR (upper panels), AKT (middle panels) and MAPK (lower panels). Total EGFR, AKT and MAPK were used as loading controls. **B**) EGF stimulates anoikis resistance of p120 knockout cell lines. Anoikis resistance was analyzed in Trp53$^{\Delta/\Delta}$-3 and two independent Ctnnd1$^{\Delta/\Delta}$;Trp53$^{\Delta/\Delta}$ cell lines in the presence or absence of EGF and Dox as indicated. Error bars represent the standard deviation of triplicate experiments *=p<0.05. **C)** Activity of downstream growth factor signaling *in vivo*. Histopathology of mammary tumors derived from *Wcre;Ctnnd1$^{F/F}$;Trp53$^{F/F}$* (left panels) and *Wcre;Trp53$^{F/F}$* (right panels) conditional mice showing p-AKT (upper panels) and p-MAPK (lower panels). Arrows and arrowheads indicate stromal and tumor cells respectively. Bars: 50µM

Table S1. Clinicopathological characteristics of 298 invasive ductal breast cancers studied for the expression of p120.

Feature	Grouping	N or value	%
Age (years)	Mean	60	
	Range	28 to 88	
Tumour size (cm)	≤2	139	46.6
	>2 and ≤5	136	45.6
	>5	18	6.0
	Not available	5	1.7
Histological Grade	1	55	18.5
	2	98	32.9
	3	143	48.0
	Not available	2	0.7
MAI (per 2mm^2)	≤ 12	135	45.3
	≥ 13	163	54.7
Lymph node status	Negative[A]	138	46.3
	Positive[B]	146	49.0
	Not available	14	4.7

([A]: negative = N0 or N0(i+); [B]:positive = ≥N1mi (according to TNM 7th edition, 2010))

Table S2. Correlation of p120 expression with clinicopathological and molecular features of invasive breast cancer.

		p120 expression		
Feature	N	Low N (%)	High N (%)	p-value
Histological grade				
1	55	13 (23.6)	42 (76.4)	
2	98	26 (26.5)	72 (73.5)	
3	143	61 (42.7)	82 (57.3)	**0.007**
MAI (per 2mm^2)				
≤ 12	135	33 (24.4)	102 (75.6)	
≥ 13	163	67 (41.1)	96 (58.9)	**0.002**
Tumour size (cm)				
≤2	139	43 (30.9)	96 (69.1)	
>2 and ≤5	136	47 (34.6)	89 (65.4)	
>5	18	6 (33.3)	12 (66.7)	0.814

Table S2. Correlation of p120 expression with clinicopathological and molecular features of invasive breast cancer. (Continued)

		p120 expression		
Feature	**N**	**Low N (%)**	**High N (%)**	**p-value**
Lymph node status				
Negative	138	43 (31.2)	95 (68.8)	
Positive	146	54 (37.0)	92 (63.0)	0.301
Perou / Sorlie classification				
Luminal	227	69 (30.4)	158 (69.6)	
HER2-driven	19	7 (36.8)	12 (63.2)	
Basal/TN	52	24 (46.2)	28 (53.8)	0.090
Hormonal receptors				
Negative	71	31 (43.7)	40 (56.3)	
Positive	227	69 (30.4)	158 (69.6)	**0.039**
ERα				
Negative	75	31 (41.3)	44 (58.7)	
Positive	223	69 (30.9)	154 (69.1)	0.099
PR				
Negative	135	53 (39.3)	82 (60.7)	
Positive	163	47 (28.8)	116 (71.2)	0.058
HER2				
Negative	259	88 (34.0)	171 (66.0)	
Positive	39	12 (30.8)	27 (69.2)	0.692
EGFR				
Negative	232	79 (34.1)	153 (65.9)	
Positive	64	21 (32.8)	43 (67.2)	0.853

Table S3. Immunohistochemistry of primary *Wcre;Trp53$^{F/F}$*; *Wcre;Ctnnd1$^{F/+}$;Trp53$^{F/F}$* and *Wcre;Ctnnd1$^{F/F}$;Trp53$^{F/F}$* mouse mammary tumors.

Genotype	Animal ID	Pathology ID	Diagnosis	*p120*	*E-cadherin*	*CK8*	*CK14*	*Vimentin*
Wcre;Trp53$^{F/F}$	941469	12SJK134	AC + SC/CS	+ (mem AC)	+ (mem AC)	+	+ (f)	+(sarc)
	949070	12SJK154	AC + SC/CS	+ (mem AC)	+ (mem AC)	+	+ (f)	+/-(sarc)
	949071	12SJK135	SC/CS	+ (cyt)	-	-	+ (f)	+
	950620	12SJK145	SC/CS	+ (cyt)	-	-	+ (f)	+
	995647	12SJK159	AC + SC/CS	+ (mem AC)	+ (mem AC)	-	+ (f)	+(sarc)
	995648	12SJK167	SC/CS	+ (cyt)	-	+	+ (f)	+/-
	1021710	13SJK001	SC/CS	+ (cyt)	-	-	+ (f)	+
Wcre;Ctnnd1$^{F/F}$;Trp53$^{F/F}$	771229	11SJK061	AC + SC/CS	+/-	+/-	+	+ (f)	+(sarc)
	772032	11SJK012	SC/CS	+/-	+	+ (f)	+ (f)	+
	772034	10SJK267	SC/CS	+	+	+	+ (f)	+
	772036	11SJK026	SC/CS	+	+/-	+	+ (f)	+
	779779	11SJK034	SC/CS	+	+	-	+	+
	785919	11SJK052	SC/CS	+	+	-	+	-
	785920	11SJK155	SC/CS	+ (cyt)	+	-	+ (f)	+
	811561	11SJK139	SC/CS	+	+	+ (f)	+	+
	811563	11SJK159	SC/CS	+	+	+ (f)	+ (f)	+ (f)
	811576	11SJK152	SC/CS	+	+/-	+ (f)	+	+
Wcre;Ctnnd1$^{F/+}$;Trp53$^{F/F}$	634482	09DER002	SC/CS	nd	-	-	-	+
	634485	09DER009	SC/CS	nd	+/- (cyt)	+	nd	-
	653684	09DER014	SC/CS	-	-	+ (f)	+ (f)	+
	749675	10SJK247	SC/CS	-	+ (cyt)	-	+	+
	757516	10SJK246	SC/CS	-	+ (cyt)	+ (f)	+ (f)	+
	771213	11SJK003	SC/CS	-	+ (cyt)	-	+ (f)	+
	785921	11SJK067	SC/CS	-	+ (cyt)	+ (f)	+	+
	788323	11SJK054	SC/CS	-	+ (cyt)	+ (f)	+	+
	795701	11SJK053	SC/CS	-	+ (cyt)	+ (f)	+	+ (f)
	805081	11SJK157	AC	-	+/- (mem)	+	+ (f)	-
	805082	11SJK173	SC/CS	-	+ (cyt)	-	+ (f)	+
	826536	11SJK170	SC/CS	-	+ (cyt)	-	+ (f)	+

f=focal, cyt=cytosol, mem=membrane, sarc=sarcomatoid cells, CK8 and CK14 show a mixed but exclusive expression pattern.

Table S4: Loss of p120 induces secretion of pro-inflammatory cytokines.

Top-21 upregulated cytokines					
Trp53$^{\Delta/\Delta}$ *versus* p120-iKD			**Trp53$^{\Delta/\Delta}$ *versus* Ctnnd1$^{\Delta/\Delta}$;Trp53$^{\Delta/\Delta}$**		
Name	**HUGO**	**Fold increase**	**Name**	**HUGO**	**fold increase**
Artemin	*ARTN*	1,7	6Ckine	*CCL21*	3,9
Betacellulin	*BTC*	2,5	BRAK	*CXCL14*	3,4
Crossveinless-2	*BMPER*	1,8	CCL28	*CCL28*	1,7
MCP-1	*CCL2*	3,1	MARC	*CCL7*	3,0
Eotaxin	*CCL11*	2,1	CCN4	*WISP1*	1,4
Galectin-3	*LGALS3*	1,8	CCR9	*CCR9*	1,7
Glut 2	***SLC2A2***	**1,9**	CTACK	*CCL27*	1,5
Granzyme B	*GZMB*	2,1	Endostatin	*COL18A1*	1,9
IL-1 alpha	***IL1A***	**1,8**	**Glut2**	***SLC2A2***	**2,8**
IL-10 R alpha	*IL10RA*	5,0	**IL-1 Alpha**	***IL1A***	**2,1**
IL-11	***IL11***	**1,6**	**IL-11**	***IL11***	**2,2**
IL-12 p40/p70	*IL12*	2,5	**IL-12 p70**	***IL12A***	**1,8**
IL-12 p70	***IL12A***	**2,2**	IL17R	*IL17R*	1,7
IL-16	*IL16*	1,7	IL-1R4	*ST2*	1,7
IL-17C	*IL17C*	9,3	IL-3R Alpha	*IL3RA*	2,5
IL-17F	*IL17F*	3,4	LIF	*LIF*	2,5
IL-4 R	*IL4R*	1,6	Soggy-1	*DKKL1*	2,8
Mip-3 A	*CCL20*	1,6	SPARC	*SPARC*	2,7
TNFRSF6	***FAS***	**2,5**	TLR2	*TLR2*	1,4
PDGF R alpha	*PDGFRA*	2,0	TNF-beta	*LTA*	1,7
Timp-1	*TIMP1*	1,6	**TNFRSF6**	***FAS***	**1,9**

Trp53$^{\Delta/\Delta}$-7;p120-iKD cells (left) were treated with Dox for 4 days. PP^{hom}-3 cells and the Dox-induced Trp53$^{\Delta/\Delta}$-7;p120-iKD cells were re-plated and cultured for 4 additional days. The conditioned medium was analyzed for cytokine production using a biotin-label-based antibody array. Shown are the top- 21 upregulated cytokines upon p120 knockdown (left table) and upon p120 knockout (right table). Fold increase indicates the relative increase in pixel intensity upon p120 loss. Cytokines marked in bold are upregulated in both the p120 knockdown and knockout cell lines as compared to Trp53$^{\Delta/\Delta}$ control cells.

SUPPLEMENTAL EXPERIMENTAL PROCEDURES

Patient material

The study population was derived from the archives of the Departments of Pathology of the University Medical Center Utrecht, Utrecht, The Netherlands and comprised 298 cases of invasive ductal carcinoma (IDC) as described (1). Histological grade was assessed according to the Nottingham scheme, and mitotic activity index (MAI) was assessed as before (2). From representative donor paraffin blocks of the primary tumors, tissue microarrays were constructed as described (1, 3). The use of anonymous or coded left over material for scientific purposes is part of the standard treatment contract with patients in The Netherlands (4). Ethical approval was not required.

Plasmids

For stable knockdown of p120, sequences directed against mouse (5' GCCAGAAGTGGTGCGAATA 3') and human (5' GCCAGAGGTGGTTCGGATA 3') p120 and a control siRNA sequence (5' TTCTCCGAACGTGTCACGTT 3') were cloned into a Dox inducible lentiviral expression system as described (5). For p120 reconstitution experiments, pEGFP-C1-p120-1A (gift from Juliet Daniel, McMaster University, Hamilton, Canada) was mutated by means of QuikChange XL site directed mutagenesis (Stratagene) using primers containing three silent mutations (forward: 5'AACTCTTATTTCAGCCAGAAGT**C**GT**C**CG**C**ATATACATTTCACTCCTTAAGG3', reverse: 5'CCTTAAGGAGTGAAATGTATAT**G**CG**G**AC**G**ACTTCTGGCTGAAATAAGAGTT3'). *EcoR*V and *Nhe*I sites were added 5' and 3' of p120-1A, using Phusion PCR (Thermo Scientific) (forward: 5'AATTGATATCATGGACGACTCAGAGGTGGAGTCGAC3', reverse: 5'TTAAGCTAGCCTAAATCTTCTGCATCAAGGGTGCTCCC3'). *EcoR*V-p120-1A-*Nhe*I was subsequently cloned into the lentiviral expression vector pLV.bc.puro (a gift from Clemens Löwik, Leiden University Medical Center, Leiden, the Netherlands). pCMV-SPORT-EGF (open biosystems) was used as template to generate the DIG-labeled EGF probe by PCR. Primers: forward: 5' GGACTTGTGCCGGTCCTGCC 3', reverse: 5' GCGCTCGAGTGGGACTTGGG 3'

Immunohistochemistry and fluorescence

Tissues were isolated, fixed in 4% formaldehyde for 48 hours, dehydrated, cut into 4µm sections and stained with hematoxylin and eosin. For single staining, fixed sections were rehydrated and incubated with primary antibodies. Endogenous peroxidases were blocked with 3% H_2O_2 and stained with biotin-conjugated secondary antibodies,

followed by incubation with HRP-conjugated streptavidin-biotin complex (DAKO). Substrate was developed with DAB (DAKO). For immunofluorescence, fixed sections were rehydrated, boiled in citrate and incubated with primary antibodies overnight. Stainings were scored as described (1). Cells were grown on cover slips and fixed in 1% paraformaldehyde/PBS for 10 minutes. Cells were permeabilized using 0.3% Triton-X100/PBS and subsequently blocked using 5% BSA (Roche). Samples were incubated with primary antibodies in 1% BSA for 60 minutes, followed by secondary antibodies for 30 minutes. DNA was stained with DAPI for 5 minutes (Molecular Probes) and cover slips were mounted onto object glasses using vectashield mounting medium (Vector laboratories).

In situ-hybridisation–IHC double staining was performed on freshly frozen tissue as described (6). Slides were hybridized overnight with DIG-labeled EGF probe as described (6). Subsequently, the slides were incubated with primary antibody F4/80. EGF probes were detected with a sheep anti- digoxigenin antibody (Roche) followed by a secondary rabbit anti-sheep antibody (DAKO). Alexa Fluor-555-conjugated goat anti-rabbit (Invitrogen) was used to detect DIG-labeled EGF probes. Samples were analyzed using a DeltaVision RT system (Applied Precision) using a 40x, 63x and 100x lens at room temperature, equipped with a CoolSnap HQ camera and SoftWorx software. Maximum projections were taken from a stack of deconvolved images.

REFERENCES

1. Vermeulen JF, van de Ven RA, Ercan C, van der Groep P, van der Wall E, Bult P, et al. Nuclear Kaiso expression is associated with high grade and triple-negative invasive breast cancer. PLoS One. 2012;7:e37864.
2. van der Groep P, Bouter A, van der Zanden R, Siccama I, Menko FH, Gille JJ, et al. Distinction between hereditary and sporadic breast cancer on the basis of clinicopathological data. Journal of clinical pathology. 2006;59:611-7.
3. Packeisen J, Korsching E, Herbst H, Boecker W, Buerger H. Demystified...tissue microarray technology. Molecular pathology : MP. 2003;56:198-204.
4. van Diest PJ. No consent should be needed for using leftover body material for scientific purposes. For. Bmj. 2002;325:648-51.
5. Schackmann RC, van Amersfoort M, Haarhuis JH, Vlug EJ, Halim VA, Roodhart JM, et al. Cytosolic p120-catenin regulates growth of metastatic lobular carcinoma through Rock1-mediated anoikis resistance. J Clin Invest. 2011;121:3176-88.
6. Klein SC, van Wichen DF, Golverdingen JG, Jacobse KC, Broekhuizen R, de Weger RA. An improved, sensitive, non-radioactive in situ hybridization method for the detection of cytokine mRNAs. APMIS. 1995;103:345-53.